Determination of rapid Deccan eruptions across the Cretaceous-Tertiary boundary using paleomagnetic secular variation: Results from a 1200-m-thick section in the Mahabaleshwar escarpment

Anne-Lise Chenet, Frédéric Fluteau, Vincent Courtillot, Martine Gérard, K. V. Subbarao

Determination of rapid Deccan eruptions across the Cretaceous-Tertiary boundary using paleomagnetic secular variation: Results from a 1200-m-thick section in the Mahabaleshwar escarpment

Anne-Lise Chenet,[1] Frédéric Fluteau,[1] Vincent Courtillot,[1] Martine Gérard,[2] and K. V. Subbarao[3]

Received 18 July 2006; revised 6 April 2007; accepted 17 December 2007; published 30 April 2008.

[1] Flow-by-flow reanalysis of paleomagnetic directions in two sections of the Mahabaleshwar escarpment, coupled with analysis of intertrappean alteration levels shows that volcanism spanned a much shorter time than previously realized. The sections comprise the upper part of magnetic chron C29r, transitional directions and the lowermost part of C29n. Lack of paleosecular variation allows identification of four directional groups, implying very large (40 to 180 m thick) single eruptive events (SEEs) having occurred in a few decades. Paleomagnetism allows temporal constraints upon the formation of 9 out of 23 thin red bole levels found in the sections to no more than a few decades; the two thickest altered layers could have formed in 1 to 50 ka. The typical volumes of SEEs (corresponding to magnetic directional groups) are estimated at 3000 to 20,000 km^3, with flux rates $\sim$100 km^3 a^{-1}, having lasted for decades. Flood basalt emission can be translated into SO_2 injection rates of several Gt a^{-1}, which could have been the main agent of environmental change. The total volume of SO_2 emitted by the larger SEEs could be on the order of that released by the Chicxulub impact. Moreover, each SEE may have injected 10 to 100 times more SO_2 in the atmosphere than the deleterious 1783 Laki eruption. The detailed time sequence of SEEs appears to be the key feature having controlled the extent of climate change. If several SEEs erupted in a short sequence (compared to the equilibration time of the ocean), they could have generated a runaway effect leading to mass extinction.

Citation: Chenet, A.-L., F. Fluteau, V. Courtillot, M. Gérard, and K. V. Subbarao (2008), Determination of rapid Deccan eruptions across the Cretaceous-Tertiary boundary using paleomagnetic secular variation: Results from a 1200-m-thick section in the Mahabaleshwar escarpment, *J. Geophys. Res.*, *113*, B04101, doi:10.1029/2006JB004635.

1. Rationale and Background

[2] Since the beginning of the Phanerozoic, life on Earth has been punctuated by a small number of discrete mass extinctions. Continental flood basalts (CFB) have been found in the case of each major mass extinction since 300 Ma [e.g., *Courtillot and Renne*, 2003]. Other flood basalts and oceanic plateaus (forming the family of large igneous provinces or LIPs) also correlate with smaller mass extinctions and oceanic anoxia events [e.g., *Rampino and Stothers*, 1988; *Courtillot*, 1994; *Wignall*, 2001] (for a recent review of occurrences and ages, see *Courtillot and Renne* [2003]). On the other hand, evidence for impact other than at the Cretaceous-Tertiary (K-T) boundary has been suggested only for the Permo-Triassic boundary, by *Becker et al.* [2004] and is hotly contested [*Farley et al.*, 2005]. *White and Saunders* [2004] concluded that the three major extinctions of the last 300 Ma occurred by the combined effects of impact and flood basalts. On the other hand, *Macleod*'s [2004] analysis of potential correlations of extinction, impact, anoxia and LIP events found that the extinction and LIP time series were the only two that were (highly) significantly correlated.

[3] The most recent and better known of the largest five mass extinctions, the K-T extinction 65 Ma ago, became the focus of unprecedented analysis following the proposal by *Alvarez et al.* [1980] that it had been caused by impact of a large extraterrestrial object. Worldwide occurrence of an exceptional iridium anomaly, observation of grains of quartz with shock features and discovery of the impact crater at Chicxulub in the Yucatan peninsula of Mexico are among a large set of evidence that impact occurred and coincided with the main K-T extinction phase (see *Smit* [1999] and *Keller et al.* [2003] for end-member views). *Bhandari et al.* [1995], confirmed by *Courtillot et al.* [2000], located the

[1] Laboratoire de Paléomagnétisme, IPGP, Paris, France.
[2] Institut de Recherche pour le Développement and IMPMC, Paris, France.
[3] Centre for Earth Science and Space Sciences, University of Hyderabad, Hyderabad, India.

0148-0227/08/2006JB004635$09.00

iridium level in intertrappean sediments in the Kutch region of India, demonstrating that both Deccan trap volcanism and impact coincided in time but, importantly, that there could be no causal connection between the two.

[4] It is likely that a large bolide impact and a flood basalt can create environmental changes which have similarities [e.g., *Courtillot*, 1999]. Both events inject dust (impact) or tephra (flood basalt), gases and aerosols, and can cause massive atmospheric pollution and hence climate change. On the one hand, impact on a crust rich in carbonates and evaporites will liberate large amounts of CO_2 and SO_2, which will be injected at and above stratospheric levels. On the other hand, flood basalts have been considered by some as major potential sources of atmospheric warming due to CO_2 [*McLean*, 1985], then by others as major potential sources of atmospheric cooling due to SO_2 [*Rampino and Self*, 2000]. Sulfur would start a cycle of sulfate aerosols with drastic climatic consequences: in the case of the K-T impact, these have been modeled by *Pierazzo et al.* [2003], who propose that climate forcing was 100 times larger than that from the Pinatubo eruption. Over a period of at least 6 years, sulfur outgassed by the impact would have led to very significant cooling at the Earth's surface.

[5] The impact of volcanism on climate and environment depends on lava eruption rate, amount and composition of gases (mainly sulfur and carbon dioxide) and altitude reached by the volcanic plume (itself a function of eruption rate). The 1991 Pinatubo volcanic eruption induced global cooling of about 0.3°C [*Bekki et al.*, 1993; *Kirchner et al.*, 1999], whereas the 1783 Laki eruption led to major climate perturbations in the northern hemisphere (exceptional warming, then cooling, and an unusual haze) [*Thordarson and Self*, 2003; *Chenet et al.*, 2005; *Oman et al.*, 2006a, 2006b]. In the case of a flood basalt, it had long been argued that fissure eruptions would not be able to inject gases at stratospheric altitudes. However, *Thordarson and Self* [1993] and [*Thordarson et al.*, 1996] have demonstrated that the 1783 Laki eruption in Iceland, which delivered 15 km^3 of basaltic lava in ~8 months, did inject large amounts of sulfur (122 Mt of SO_2) in the lower stratosphere (10–13 km). *Stothers et al.* [1986] calculated convective plume height as a function of eruption flux rate and concluded, in the case of the 15 Ma Roza flow field eruption (one of the largest units in the Columbia River flood basalt), that stratosphere-high eruption plumes should have been produced, leading to widespread sulfur distribution and global climate change. The associated fire fountains would have exceeded 1.5 km in height, and the powerful convective columns induced by eruption dynamics could have participated in propelling a significant amount of volatiles to the lower stratosphere [*Thordarson et al.*, 1996; C. Jaupart, personal communication, 1993]. A single flow from a flood basalt can be more than 2 orders of magnitude larger than the Laki (in excess of 1000 km^3 according to recent work on the Roza flow field in the Columbia River traps by *Self et al.* [2006]), and hundreds of such flows are stacked in a single LIP, so that stratospheric injection and the potential for a global environmental effect of a LIP are not any more in doubt. *Self et al.* [2006] argue that such huge lava flows can be emplaced in as little as a few years. This would imply lava effusion rates up to 100 $km^3\ a^{-1}$ (almost an order of magnitude larger than the 1783 Laki eruption rate, and with a duration up to 10 times longer). And yet, the Roza flow field is not linked to a known extinction event. Therefore, if LIPs are associated to mass extinctions, the total number and detailed time sequence of flows must be viewed as a probable trigger of the climatic catastrophe.

[6] The main way in which the effects of an impact, a single large flow, or a full-scale LIP can be distinguished is their time signature. Impact of an extraterrestrial object on Earth is quasi-instantaneous, whereas emplacement of a full-fledged flood basalt involves timescales thought to range from 10^4 to 10^6 years, based on geochronological dating and magnetostratigraphy. The long duration of a flood basalt province (i.e., trap) emplacement relative to impact has been repeatedly advocated to question the disruptive potential of volcanism regarding mass extinctions [e.g., *Erwin*, 2004; W. Alvarez, personal communication, 1993], despite the fact that the more severe mass extinctions do coincide with emplacement of large flood basalts (at the best currently available time resolution [*Courtillot and Renne*, 2003]). So, how could a 1-Ma-long geological event lead to the "abrupt" disappearance of numerous species? When would (and how could) such large lava flows cause mass extinctions? In particular, how does the Deccan eruption relate to the K-T crisis? It has been proposed (in a qualitative way by *Courtillot et al.* [1986] and in a quantitative way by *Thordarson* [2004], *Chenet et al.* [2005], *Courtillot and Thordarson* [2005], *Self et al.* [2006], and *Fluteau* [2006]) that the Deccan Traps actually comprise a succession of a rather small number of larger volcanic pulses (which we call single eruptive events or SEE hereafter), formed in a relatively short time. But in order to model the consequences of a trap, the "forcing function" must be known far more accurately, requiring dating of eruptive episodes (that is their duration and intervals between SEEs) with up to 10^2 to 10^3 year resolution!

[7] With this goal in mind, we have initiated a field and laboratory program in order to better constrain the time history of the Deccan lava pile, mainly based on a restudy of the paleomagnetism of the complete flow sequence. We hoped to be able to identify groups of lava flows with statistically similar magnetic directions, indicating short eruption times (based on the typical time rates of geomagnetic secular variation). Our program was launched as a cooperation between French and Indian teams in 2003, based on extensive fieldwork by one of us (K. V. Subbarao) and his students [e.g., *Subbarao et al.*, 2000]. A complementary program had been undertaken by a team from the Open University in the United Kingdom, led by S. Self and M. Widdowson, in the frame of A. Jay's thesis, now completed [*Jay*, 2005], and a collaboration was established. This first paper reports mainly our paleomagnetic results from a 1200-m-thick section (and a shorter section 20 km away) located in the upper part of the Deccan stratigraphy. Subsequent work will report results from sections located to the north in the lower half of the Deccan stratigraphy.

2. Geological Background and Methodology

2.1. An Overview of the Deccan Traps

[8] The Deccan Traps in India are one of the largest continental flood basalt provinces (CFB) on Earth (west central India; 20°N–16°N, 70°E–79°E; Figures 1a and 1b).

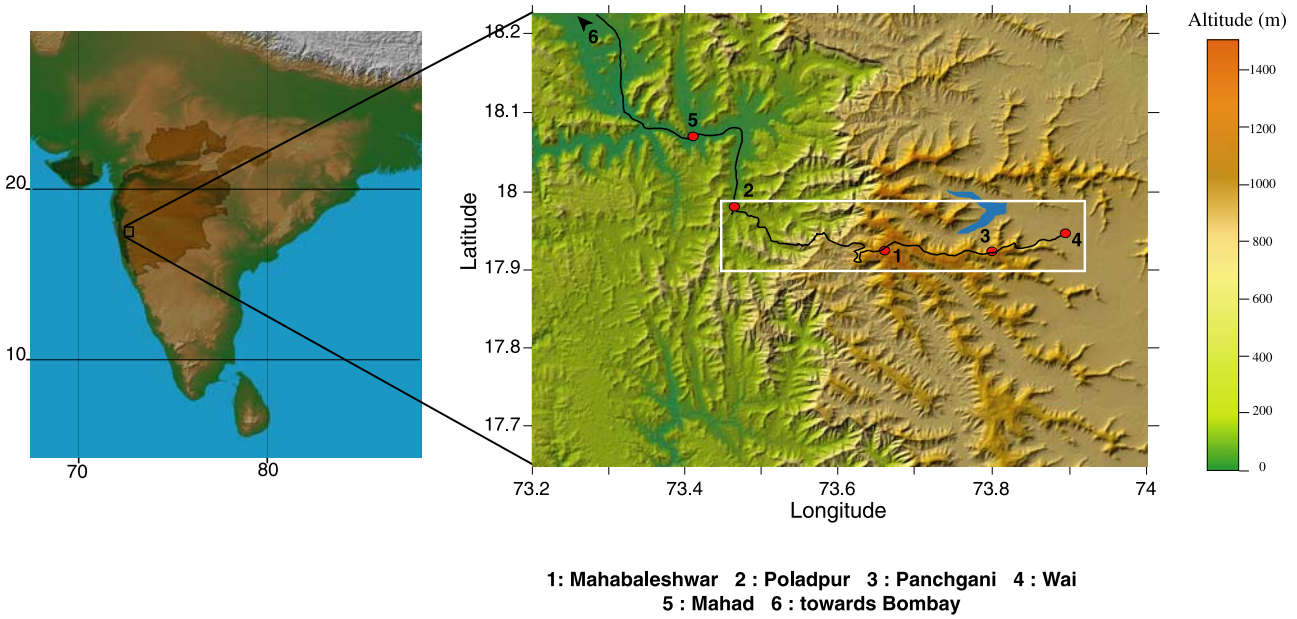

Figure 1a. (left) Map of India with present extent (darker brown) of the Deccan Traps. (right) Digital elevation model of the Western Ghats in the area of the Mahabaleshwar Plateau. White rectangle indicates study area with two sections from Mahabaleshwar to Poladpur and Wai to Panchgani. Red circles correspond to cities and villages.

The volume of the lava, prior to continental breakaway of the Seychelles microcontinent and to erosion, probably far exceeded a million cubic kilometers, erupted in only a million years or less, straddling the iridium-defined K-T boundary [*Courtillot et al.*, 1986]. Extensive previous geochemical work (coupled to petrologic and stratigraphic analysis) in the Western Ghats [*Beane et al.*, 1986; *Devey and Lightfoot*, 1986; *Mitchell and Widdowson*, 1991], complemented by magnetostratigraphic studies [*Vandamme et al.*, 1991; *Vandamme and Courtillot*, 1992], has allowed a chemomagnetostratigraphy of the traps. The Deccan Main Province, which represents about 80% of the total present-day volume, has been divided stratigraphically into twelve formations and three major subgroups: Kalsubai (∼2000 m thick), Lonavala (∼525 m thick) and Wai (∼1100 m thick), going from older to younger [*Cox and Hawkesworth*, 1984, 1985; *Beane et al.*, 1986; *Devey and Lightfoot*, 1986; *Subbarao et al.*, 1994; *Jerram and Widdowson*, 2005] (Figure 2). Each formation is characterized by accumulations of large composite subhorizontal tholeiitic flows with varying thicknesses, and chemical and mineralogical composition.

[9] This body of work also enabled the overall structure of the trap body to be elucidated, revealing a major north-south trending axis of flexure, with small eastward flow dip to the east of the Main Province escarpment and more pronounced westward dip to the west, in the direction of the Arabian Sea coast. In addition, flows have a small regional dip to the south. *Jerram and Widdowson* [2005] have most recently reconstructed the structure of the Deccan Traps as a stack of staggered lenses, where older formations outcrop in the north near Nasik and younger ones in the south near Mahabaleshwar (Figure 2a). Much of the Deccan volcanic pile (which has a combined thickness of about 3500 m) appears as a flat, elevated plateau (the Maharashtra Plateau), with an escarpment near the western margin, 50 to 100 km inland of the coast. This escarpment, called the Western Ghats after the Hindi term for "steps", is interpreted as a receding erosional trace of the original normal fault system linked to continental breakaway of the Seychelles [*Widdowson and Cox*, 1996].

[10] Extensive geochronological dating, originally based on the K-Ar method, and more recently on more modern ^{40}K-^{40}Ar and ^{39}Ar-^{40}Ar techniques, has been reviewed at various stages [*Courtillot et al.*, 1986, 1988; *Duncan and Pyle*, 1988; *Vandamme et al.*, 1991; *Venkatesan et al.*, 1993; *Hofmann et al.*, 2000; *Pande*, 2002]. Comparison of absolute ages provided by different laboratories at different locations and times (even when they basically use the same technique, i.e., Ar-Ar) requires careful checking of monitors and other parameters. Accordingly, such interlaboratory comparisons can rarely be done at the sub-1-Ma level [see *Courtillot et al.*, 1988; *Duncan and Pyle*, 1988; *Venkatesan et al.*, 1993; *Féraud and Courtillot*, 1994; *Venkatesan et al.*, 1996; *Hofmann et al.*, 1997; *Courtillot et al.*, 2000; *Hofmann et al.*, 2000; *Kamo et al.*, 2003; *Knight et al.*, 2003; *Riisager et al.*, 2005]. The duration of Deccan volcanism has also been estimated based on magnetic stratigraphy [*McElhinny*, 1968; *Pal*, 1969]. Several polarity transitions, in particular a reverse-to-normal polarity transition in the area of Mahabaleshwar, have been found in the Deccan Traps, suggesting that lava emplacement took place over an interval of time much longer than the time constant of secular variation, but shorter than that of continental drift [*Wensink and Klootwijk*, 1971].

[11] On the basis of joint analysis of paleomagnetic, Paleontological, and geochronological data, *Courtillot et al.* [1986] suggested that volcanic activity lasted less than 1 Ma and spanned the K-T boundary. This was strengthened by additional Ar data of *Courtillot et al.* [1988] and *Duncan*

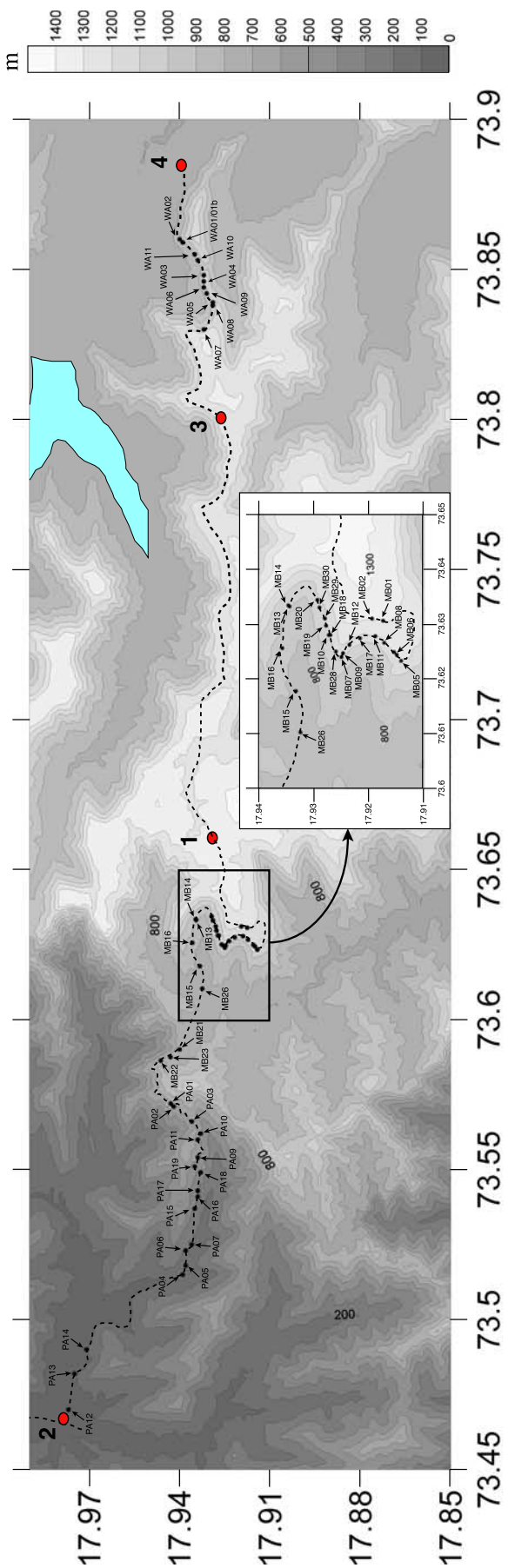

Figure 1b. Details of site distribution along the two road sections.

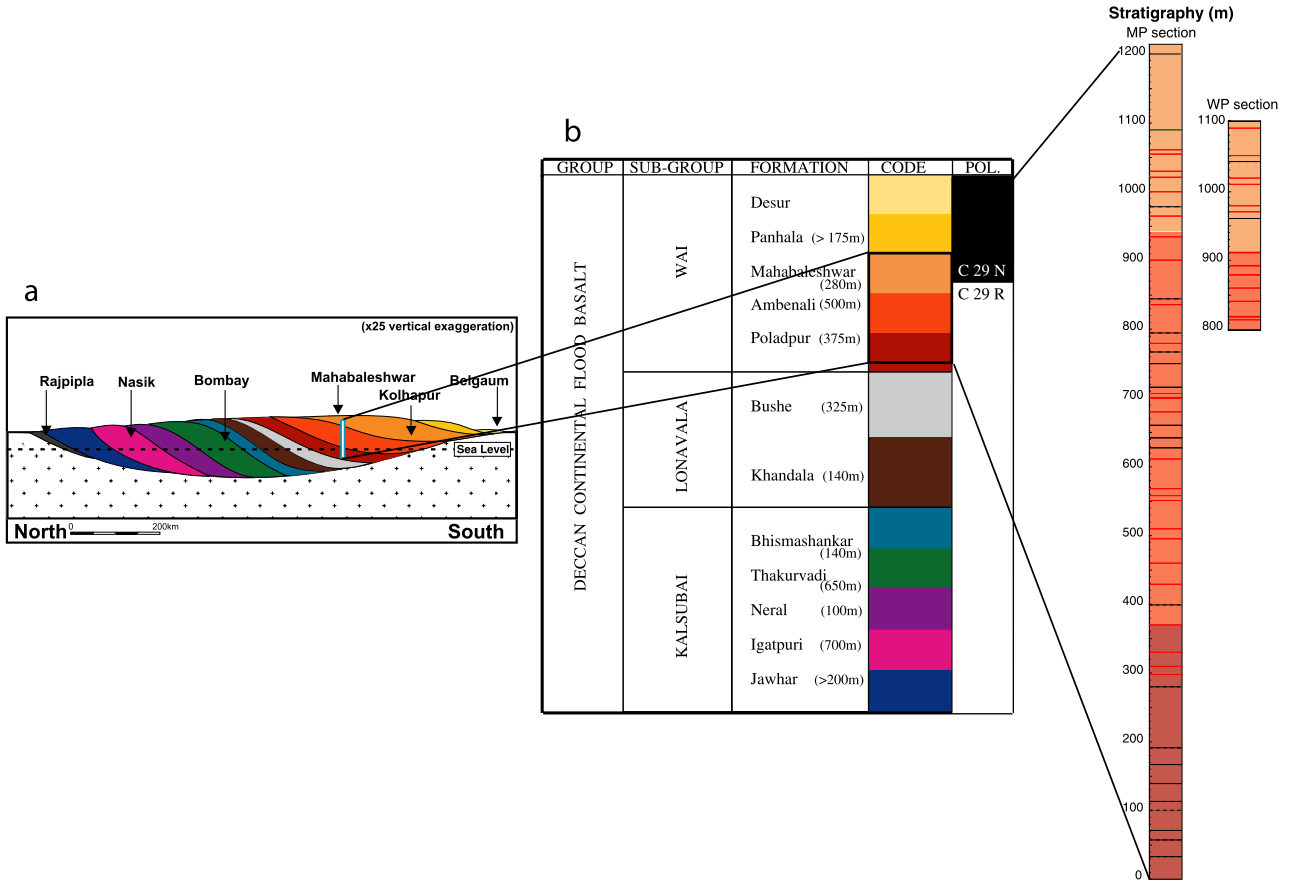

Figure 2. (a) Schematic view of the 12 formations comprising the Deccan Traps in the Western Ghats in the shape of staggered lenses overstepping from north to south (after data from *Jerram and Widdowson* [2005]). (b) Division of the Deccan Traps into three chemical subgroups and 12 formations. Our study focuses on the Poladpur, Ambenali, and Mahabaleshwar Formations, which outcrop along the 1200-m-thick Mahabaleshwar-Poladpur (MP) ghat section and 300-m-thick Wai-Panchgani (WP) section.

and Pyle [1988]. But *Venkatesan et al.* [1993], followed in a recent review by *Pande* [2002], proposed that volcanism started in Cretaceous chron C31n (~68.7 Ma), and ended in Danian (Cenozoic) chron C28n (~62.1 Ma), i.e., lasted more than 6 Ma, with several periods of quiescence, the most intense SEE occurring at 66.9 ± 0.2 Ma, before (and not at) the K-T boundary (dated at about 65.0 Ma). *Hofmann et al.* [2000] collected and analyzed samples from close to the bottom and top of the main lava pile in the Western Ghats. They found a mean age of 65.8 ± 0.7 Ma for five flows near the base of the section and 65.5 ± 0.2 Ma for a dike crosscutting the Poladpur formation (recalculated relative to an age of 523.1 Ma for the MMhb-1 standard [*Renne et al.*, 1998; *Chenet et al.*, 2007]), implying that at least 1800 m out of the 2500 m composite trap section were erupted in less than 1 Ma close to the K-T boundary. A new K-Ar dating campaign has been undertaken in the frame of the present study and is reported elsewhere [*Chenet*, 2006; *Chenet et al.*, 2007]. The geomagnetic polarities recorded in the Western Ghats would imply that ~80% of the volume of the traps erupted during reversed chron C29r (~65.6 to ~64.7 Ma, following *Cande and Kent* [1995]) and the early part of C29n. C29r lasted ~800 ka, leading to a duration of emplacement for the (reversed) bulk of the lava less than 1 Ma and potentially straddling the Cretaceous-Tertiary boundary. More recent paleomagnetic studies to the north of the Narmada valley have retrieved the N-R-N succession proposed by *Courtillot et al.* [1986], confirming that volcanism in that northern area started in C30n [*Khadri et al.*, 1988, 1999].

2.2. Architecture of the Ambenali Ghat

[12] We focused our study on the upper part of the Deccan Traps, namely on three formations of the Wai subgroup: Mahabaleshwar (M'war; ~280 m), Ambenali (~500 m) and Poladpur (~375 m) (Figure 2). The 1200-m-thick Ambenali Ghat (or Mahabaleshwar-Poladpur (MP) Ghat) section corresponds to approximately one third of the total trap thickness. The Ambenali Formation alone likely has a volume similar to that of the entire Columbia River CFB [*Self et al.*, 2006]. We sampled these formations in the Mahabaleshwar plateau, where a detailed stratigraphy was available (see field excursion guide, edited by *Subbarao et al.* [2000]). The distinction between formations is based on flow type, rock texture and chemistry [*Najafi et al.*, 1981; *Mahoney et al.*, 1982; *Cox and Hawkesworth*, 1985; *Beane et al.*, 1986; *Devey and Lightfoot*, 1986; *Bodas et al.*, 1988; *Subbarao and Hooper*, 1988; *Khadri et al.*, 1999]. The Ambenali Ghat section is known to contain the C29n/C29r

magnetic reversal [*Wensink and Klootwijk*, 1971; *Kono et al.*, 1972; *Jay*, 2005].

[13] The detailed mesoscale architecture of the 1200-m-thick MP ghat section has recently been restudied by *Jay* [2005] using lithological, petrographic, volcanological and geochemical constraints and has been complemented by our own observations. We recall that a lava unit is a nongeneric term attributed to each outcrop observed in the field. Following the generic terminology of *Self et al.* [1997], a single lava unit, also named a flow lobe, is defined as a cooling unit bound by quenched margins on all sides, irrespective of its size or whether it is bound by coherent pahoehoe or rubbly margins. A very large flow lobe, as often occurs in the Deccan, is also called a sheet lobe. A single outpouring of lava comprising several lava units, which is typically formed after a short time of quiescence, is called a lava flow unit. A number of lava flow units define a flow field. On the basis of observations of recent volcanism, detailed analysis of large flows in the Columbia River and Deccan flood basalts, and physical volcanology considerations, Self and coauthors [*Self et al.*, 2006; *Thordarson and Self*, 1998] have shown that a single flow field with lava volumes up to several thousand cubic kilometers could be emplaced over timescales of decades, probably not much exceeding a century. This corresponds to a single eruptive event, which is also a large cooling unit. Flow structures in the MP ghat section are similar to those found in the Columbia River Basalt or Hawaii [*Jay*, 2005; *Self et al.*, 2006, 2008]. *Jay* [2005] identified 49 successive lava units forming 29 flow fields, according to the number of sheet lobes and the exposure.

[14] Lava flows are bounded either by direct contacts (implying a short time between flows, or removal of alteration products, or climate not conducive to alteration) or by red weathered horizons, named red boles (RB). Various interpretations have been proposed for the generation of RBs. On the basis of geochemical analysis, they could be sediments, weathered basalts, weathered pyroclasts, soils, or metasomatized or baked zones [*Shepard*, 1963; *Inamdar and Kumar*, 1994; *Wilkins et al.*, 1994; *Mohapatra and Nair*, 1996; *Widdowson et al.*, 1997; *Salil et al.*, 1997; *Khadkikar et al.*, 1999; *Sethna*, 1999; *Singh*, 2000; *Ross et al.*, 2005; *Sayyed et Hundekari*, 2006; *Gosh et al.*, 2006]. A fuller analysis of RBs is beyond the scope of this paper and will be presented in another paper; we only provide elements on how red boles are likely formed, based on our sampling of interflows. The less developed RBs, only a few centimeters thick, consist of red silty clay below an altered (centimeter thick) upper flow sole. Sometimes the reddish clay occurs only within fractures in the upper blocks of the lower lava flow. These thick RBs (up to 1 m thick) are characterized (over a few tens of centimeters) by red compact silty clay, underlying an altered upper flow base, grading to reddish pink silty clay with friable vesicular relics of basalt blocks ($\sim$1 m). The lower lava flow is altered over less than 1 m, grading from red-brown clay-jointed blocks to massive altered blocks, suggesting downward decreasing alteration (decreasing occurrence of clay minerals and vacuole infillings). There are few mineralogical (and fewer micromorphological) data for these RBs in the literature. Our study indicates smectites, zeolites, and hematite [*Gérard et al.*, 2006]. The red clayey horizons or joints are characterized by mixed hematite and smectites or smectite microgeodes. Voids or fissures are coated with smectites, and/or infilled by zeolites and Mn oxides throughout the altered lava relic blocks of the lower flow. Maximum alteration is observed at the altered sole of the upper lava flow, with a centimeter-thick lithified Fe-beidellite rich zone overlying the red silty clay. From the top to the base of the profile, a trend from beidellite to nontronite occurs in clay minerals. The red color of the silty clay is due to hematite.

[15] Descriptions of paleosols or buried soils [*Retallack*, 1991: *Sheldon*, 2003, 2005; *Gérard et al.*, 2007] are generally supported by pedogenic morphology, root traces or plant fossils, or organic matter content. But postburial alteration may have erased these signatures. One of the most important is the morphology of the contacts (sharp upper contact and gradational download). Specific paleosols have been described in similar reddened interflows of the Columbia River Basalt Province [*Sheldon*, 2003]. We found no root traces or organic matter. Upper contacts only appear to be sharp, due the red color and difference between a lithified horizon and friable silty red clay. Another characteristic is the grain size change due to burial dehydration and recrystallization/coarsening of iron hydroxides and oxides [*Retallack*, 1991], resulting in the formation of hematite. On the basis of micromorphological and mineralogical analysis, the RBs of the MP section appear to be the result of a hydrothermal deuteric alteration process, similar to that observed in the Massif Central [*Mélières and Person*, 1978]. The deuteric mechanism is the alteration of the chilled sole of the upper flow due to its own last liquid water fraction, occurring in a few years. The relic of the altered chilled sole is the beidellite lithified base of the upper flow. In the case of the thick RBs, the lower flow is more weathered (e.g., hydrated): a large autoclave is created by the upper flow, which vaporizes the fluids of the underlying hydrated lower flow, creating a forced hydrolysis [*Gérard et al.*, 2006]. Saprolitic RBs have also been described by *Widdowson et al.* [1997]. Hydration of the glass, associated to cooling, generates new hydrothermal smectites; this is also observed in seamounts [*Schöps et al.*, 1993]. Thin red boles (which are not developed soils) can be observed between lava units. Although timing of development is not well constrained, thick red boles are not observed within a flow field, which can be emplaced in a time not exceeding a century [*Thordarson and Self*, 1998; *Self et al.*, 2006], but, as will be seen in this paper, thin ones can.

2.3. Sampling Strategy

[16] We sampled 45 sites along the Mahabaleshwar-Poladpur ghat section from the well-exposed lava flows (from 17.98°N, 73.47°E to 17.92°N, 73.63°E) (Figures 1a, right, and 1b). Below 50 m altitude, lava units are assigned to the Bushe formation [*Devey and Lightfoot*, 1986; *Jay*, 2005]. Outcrops consist of (0.1 to 2 m thick) pahoehoe lobes with ropey flow tops and pipe vesicles [*Subbarao et al.*, 2000; *Jay*, 2005]. Because of poor exposure, we sampled only one paleomagnetic site (PA12), close to the town of Poladpur. Geochemical results on these samples (C. Pellan, personal communication, 2006) indicate a trace element pattern which is clearly different from the Bushe type but identical to the overlying Poladpur Formation. It is

therefore likely that the Bushe-Poladpur transition occurs below 20 m altitude along the section.

[17] The Poladpur Formation (originally thought to occur between 60 and 333 m; revised here to 20 and 368 m; the poor exposure between 333 and 368 m did not allow sampling) consists of 14 partially exposed lava units, which reveal a succession of several sheet lobe cores with typical characteristics, such as wide columnar joints and moderately vesicular lava. Despite low-quality exposure, four red horizons and changes in petrography allow one to conclude that these probably belong to different sheet lobes, and possibly different flow fields [*Jay*, 2005]. Eleven paleomagnetic sites (PA12 to PA18, not numbered in stratigraphic succession) were collected in the exposed units (Figure 1b).

[18] The Ambenali Formation (368–934 m) is the thickest in the whole ghat along this section. Exposures display several sheet lobes with columnar joints which are well defined by contacts with flows immediately above and below, with vesicles indicating the upper (crust) zone of a sheet lobe or the presence of red boles. One of the 16 observed red boles is more developed and has been named the "Big Red Bole". This 70-cm-thick red silty horizon overlies a couple of meters of altered basalt (N17°57.042′, E73°34.988′, at the altitude of 693 m, visible at that level for about 2 km) [*Subbarao et al.*, 2000; *Jay*, 2005; *Gérard et al.*, 2006]. This is the main evidence for a significant period of quiescence between two volcanic eruptions. The other red, altered profiles are about 10 cm thick or even less and all rather similar. We have sampled 17 paleomagnetic sites in well exposed lava units (PA19 to MB20; Figure 1b).

[19] An increase in the $^{87}Sr/^{86}Sr$ and Ba/Y ratios and in the amount of lithophile elements in basalt composition indicates passage to the Mahabaleshwar Formation chemotype (above 934 m [*Cox and Hawkesworth*, 1985]). However, the precise location of the contact between the Ambenali and M'war formations is not visible in the field. Sheet lobes and highly mafic flows characterize this formation. They can be grouped in flow fields. Flow contacts are often undulating and six red boles were observed, with a thicker one at the altitude of 965 m. Two sheet lobes are separated by a green-grey bole at 1090 m (20-cm-thick silty bed on 120 cm of altered formation; N17°54.973′, E73°37.512′), which becomes laterally thinner and reddens northward. Such greenish boles have been described in the Pune region [*Widdowson et al.*, 1997; *Sayyed and Hundekari*, 2006; *Gosh et al.*, 2006] suggesting eolian ash or pyroclastic deposits. The mineralogy of the green silty clay is different from that of the red boles: smectite, ilmenite and cristobalite account for the green color. Higher SiO_2 concentration confirms silicification; pyroclastic relics were noticed in thin section. The lower flow displays a saprolitic profile. The major volcaniclastic deposits in the Deccan Traps are rather rare and essentially located in the Mumbai region [*Cripps et al.*, 2005; *Ross et al.*, 2005]. We have chosen to oversample the M'war Formation (17 sites (MB30 to MB02) over only 250 m in height), due to occurrence of transitional directions, with a polarity change variously placed between 940 and 963 m [*Kono et al.*, 1972; *Jay*, 2005]. From 1183 m up to 1200 m, massive, poorly vesicular lava is well exposed. But there is almost no exposure from 1204 m to the top of the ghat at 1290 m; highly altered lava is visible between 1252 and 1254 m and a well developed red bole at 1215 m (N17°55.133, E73°37.811). Because of strong weathering, we did not sample the top of the Mahabaleshwar plateau, but we sampled two sites below, MB04 and MB02 at ∼1190 and ∼1200 m (Figure 1b).

[20] A second section was sampled east of M'war along the Wai-Panchgani (WP) road (Figure 1b), in order to provide complementary access to the Ambenali and Mahabaleshwar formations and to constrain the lateral extent of lava flows. *Jay* [2005] defined 18 distinct sheet lobes and 16 flow fields along this section, between 766 and 1220 m altitudes (below the laterite cap of the Panchgani Tableland, latitude 17.93°N, longitude 73.83°E). The Ambenali Formation (visible from 766 to 915 m) displays a number of flow fields, consisting of rather aphyric sheet lobes, generally separated by red boles. We observed four well-developed red boles. Two of them (at 928 m, N17°55.928′, E73°51.030′ and 892 m, N17°56.091′, E73°51.257′) have a 20-cm-thick red silty layer within a 120-cm altered profile. The two others occur at 832 m (N17°56.485′, E73°51.750′) and 872 m (N17°56.270′, E73°51.433′). The thin red boles found in this section are generally formed on breccia. Four paleomagnetic sites (WA02, WA01, WA11 and WA10) have been sampled in the Ambenali Formation. From 915 to 1089 m, basalts have the geochemical characteristics of the M'war Formation, with a succession of sheet lobes, red weathered layers and flow fields. The top of the upper flow of this section is highly weathered (soft pale grey layer). We sampled seven sites (WA03 to 07).

[21] Thus, 45 paleomagnetic sites were sampled in 36 well-exposed lava units over an altitude range of about 1200 m along the MP section and 11 sites in the 8 well-exposed lava units between altitudes of 834 and 1009 m along the WP section (Figure 1b). There was often (but not always) only one such site per lava unit. But whenever possible (very thick and well-exposed flows) up to three sites were collected from the bottom, center and top.

[22] Samples (between 8 and 13 cores per site, usually distributed horizontally along a ∼50 m length of the roadside) were collected with a portable gasoline-powered drill and each standard 2.5-cm-diameter core was oriented by both magnetic and sun compass. These two methods are in good overall agreement, with a mean angular anomaly of ∼−0.5° and a standard deviation of ∼6.0° for 428 samples with both solar and compass orientations. This is indistinguishable from the Present field (IGRF: D = −1.2°). Because of cloudy weather, six sites were oriented using only magnetic compass. Nevertheless, the corresponding site mean directions are fully consistent with others. The positions of each site were measured using a GPS. Special attention was given to elevation. For example, along the Ambenali section, the differences between our GPS readings and those of *Jay* [2005] at the same sites is as much as 10 m. We compared the elevations of all sampled sites with those found on the (horizontally) nearest grid point of the Shuttle Radar Topography Model (SRTM2, NASA [*Rodriguez et al.*, 2005]). The mean horizontal distance of our sites to grid points is 30 m and their RMS elevation differences are ∼10 m, which is an upper bound on the uncertainty. These values are in the range of uncertainties linked to the GPS and SRTM2 resolutions and to the actual distances between sampling and grid points.

2.4. Paleomagnetic Measurements and Magnetic Mineralogy

[23] One core per site was analyzed respectively by detailed stepwise thermal and alternating field (AF) demagnetization. In most cases, the characteristic component was better isolated with thermal demagnetization. Samples were demagnetized using an average of 15 demagnetization steps. All magnetic measurements were carried out in the shielded room at Institut de Physique du Globe de Paris (France), using a JR-5 spinner magnetometer. Magnetic susceptibility was monitored after each temperature step with a Kappabridge KLY 2, in order to detect possible mineralogical changes. Vector demagnetization diagrams [*Zijderveld*, 1967] for each sample were analyzed using principal component analysis [*Kirschvink*, 1980]. Site-mean directions were calculated using *Fisher* [1953] statistics or intersections of remagnetization circles [*Halls*, 1978]. Analysis used *Cogné*'s [2003] Paleomac package. Because dips of the lava flows were always very small, and actually not detectable (less than 1°) at the scale of our sites, flows were considered as horizontal and results were therefore not tilt-corrected.

[24] Figure 3 displays typical examples of demagnetization behavior, which can generally be assigned to one of three types. Core MB0807 shows an example of a low-coercivity (10 mT, 300°C) secondary component, which is generally in the direction of the Present geomagnetic field. A single characteristic component with normal polarity is then clearly isolated, with almost no overlap between the coercivity or temperature spectra of the two components. The characteristic component heads to the origin in the thermal demagnetization diagram, whereas it fails to do so in the AF demagnetization (by a small amount), indicating the remaining presence of a harder coercivity remagnetization. The highest unblocking temperature slightly above 600°C could indicate the presence of some (titano-) hematite, but the main component is clearly carried by a low-Ti titanomagnetite. This has the same direction as the main one and is therefore also acquired at the time of lava cooling. The two demagnetization techniques agree in terms of component directions. Core PA1804 has reversed polarity and shows some curvature, implying overlap of two components of magnetization. However, above 515°C the demagnetization diagram becomes linear and heads to the origin. The AF diagram also heads to the origin, although more than a third of the original NRM remains at 100 mT. The highest unblocking temperatures are also above 620°C. Core PA0804 is an example of the lower quality demagnetization behavior. In this case, AF demagnetization turns out to be a better technique to isolate a reliable direction for the characteristic component. The unblocking temperatures are consistent with low-Ti titanomagnetite.

[25] Further rock magnetic experiments specify the properties of magnetic carriers in more detail. Hysteresis parameters of samples plot within the pseudosingle-domain region on a Day diagram [*Day et al.*, 1977], with ratios of saturation remanent magnetization to saturation magnetization between 0.05 and 0.31 and ratios of coercive force over coercivity of the remanence between 1.7 and 3.4. There is no systematic evolution of these parameters as a function of stratigraphic order.

[26] Thermal experiments using an AGICO KLY 3 Kappabridge show similar behavior for samples from all formations. The maximum unblocking temperature is generally close to 550°C, confirming that magnetization is carried by a low titanium titanomagnetite (with x parameter on the order of 0.05 according to *Dunlop and Özdemir* [1997]). Generally, we observe an increase in susceptibility upon heating up to 450–500°C, and irreversible behavior with lower values upon cooling. Magnetic experiments reveal the presence of alteration products, mainly in the lowermost and uppermost parts of the section (22 to 290 m, and 1000 to 1210 m) and at six (irregularly distributed) additional sites between 898 and 474 m. These more weathered samples likely contain titanomaghemite (unblocking temperature ~350°C), which seems to be the result of low-temperature oxidation of titanomagnetite. Following *Dunlop and Özdemir* [1997], CRM due to maghemitization of titanomagnetite is indistinguishable from the original remanence. Although our samples are in the pseudosingle-domain (PSD) range, weathered and unweathered cores show the same behavior, giving some confidence in results from even the more weathered samples. Several sites (MB10, 18, 15, 23 and 26, and PA03) show very stable and reversible behavior indicating titanomagnetite (only) mineralogy. The Koenigsberger (Q) ratios range from 0.7 to 8.6. All Q ratios remain in the same range, confirming the preeminence of the remanence, except for a possible anomaly at site PA03 (Q = 27). In any case, this site shows no evidence of having been struck by lightning.

[27] This study of magnetic mineralogy along the 1200-m-thick MP section shows no significant trend in magnetic parameters or behavior throughout the different formations, in contrast with the geochemical criteria (Ba/Y, Zr/Nb, Sr and Ba versus altitude) which allow these formations and their boundaries to be determined [*Jay*, 2005, and references therein]. At a small spatial scale, magnetic mineralogy is homogeneous and does not allow us in itself to constrain magmatic subunits or SEEs.

[28] Changes in magnetic mineralogy within paleomagnetic sites are indicative of the degree of basalt weathering within a given flow. In addition, several flows contain zeolites (authigenic minerals related to hydrothermal fluid circulation). The age of hydrothermalism is poorly constrained, and probably relates to shallow burial. It should not have recorded a much different magnetic direction (given the timescale of secular variation). If, on the other hand, fluid circulation occurred long after lava emplacement, the magnetic remanence could be influenced significantly. We have tried to avoid this risk by sampling only the least altered flows with minimal amounts of zeolites. Because of very extensive previous paleomagnetic and rock magnetic experience with these Deccan lavas, further rock magnetic and paleomagnetic experiments were not deemed necessary [e.g., *Vandamme et al.*, 1991]; additional material is provided by *Chenet* [2006].

3. Paleomagnetic Results

3.1. Mean Directions and Polarity Stratigraphy in the M'war-Poladpur Ghat Section

[29] The full data are synthesized in Table 1 and are shown in Figure 4 as a stratigraphic log of declination and inclination and in Figure 5 in stereographic projection. The behavior of our samples upon thermal demagnetization is

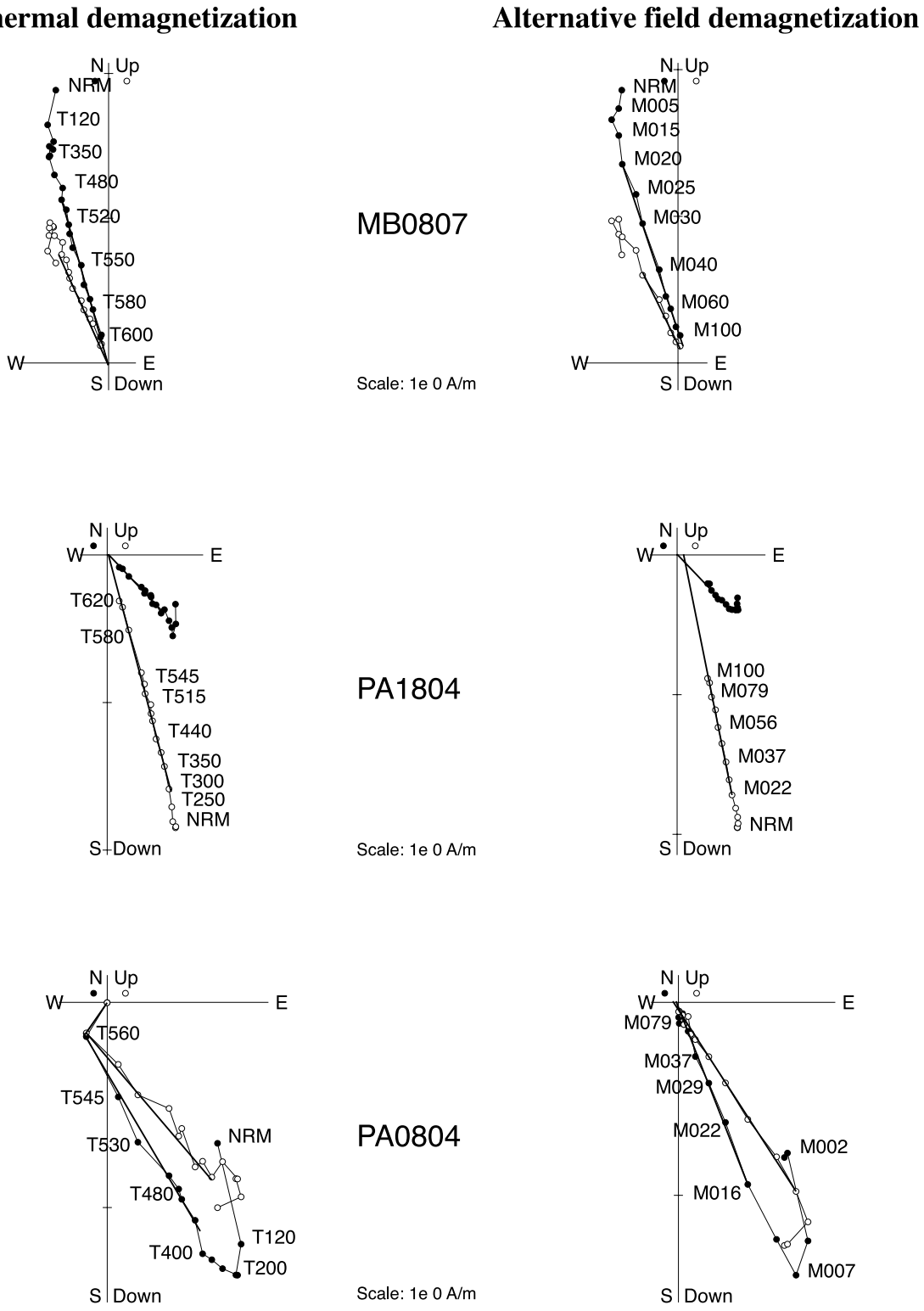

Figure 3. Three examples of orthogonal projections of (left) thermal (T) and (right) alternating field (M) demagnetizations of representative pilot samples (see text). Solid (respectively open) circles in orthogonal projections correspond to the N-S/E-W (respectively N-S-vertical) planes.

generally quite uniform: stepwise thermal demagnetization isolates a low-temperature component (LTC) (< 250°C) with a mean direction D = 0.1 ± 3.0°, I = 28.6 ± 3.4° (n = 224, α_{95} = 3.4°). This is between the Present (IGRF, I = 23.5°) and mean dipole (I = 32.9°) directions, and consistent with the idea that the LTC is a recent viscous normal overprint. The high-temperature component (HTC) (>300°C) is almost always directed toward the origin, and is taken to be the

Table 1. Paleomagnetic Results for the Mahabaleshwar-Poladpur Ghat Section[a]

Site	DG	Altitude (m)	*n*/N	Dg (deg)	Ig (deg)	κ	α_{95} (deg)	dDg	Slat (deg)	Slon (deg)
				Mahabaleshwar Formation						
MB02		1210	10/10	331.7	−17.9	127.3	4.3	4.52	17.92	73.631
MB04		1190	10/10	343.6	−39.9	15.1	12.9	16.91	17.917	73.630
MB05		1110	7/9	344.6	−47.1	211.5	4.6	6.76	17.914	73.623
MB06		1099	6/10	346.6	−42.3	26.7	14.7	20.06	17.915	73.624
MB07		1090	6/9	344.1	−36.4	53.3	10.3	12.83	17.915	73.625
MB08		1080	10/10	345.5	−39.3	125.0	4.3	5.56	17.917	73.627
MB11		1070	10/10	348.9	−39.3	446.0	2.3	2.97	17.919	73.628
MB12		1060	10/10	349.2	−43.6	64.3	6.1	8.43	17.922	73.627
MB17		1032	11/11	346.3	−48.2	124.8	4.3	6.45	17.921	73.670
MB09		1030	8/8	355.0	−46.4	180.4	4.2	6.09	17.925	73.625
MB04–MB09	*DG6*		*6/9*	*348.2*	*−44.0*	*289.0*	*3.9*		*17.0918*	*73.631*
MB27		1017	9/9	317.7	−73.5	16.1	13.6	55.88	17.917	73.617
MB28		1007	10/10	266.6	−69.8	258.0	3.0	8.71	17.926	73.625
MB10		990	11/11	268.0	−70.4	612.1	1.9	5.67	17.927	73.628
MB19		989	12/12	269.3	−70.8	184.0	3.2	9.77	17.928	73.890
MB18		985	12/12	272.1	−72.1	320.7	2.4	7.83	17.927	73.628
MB28–MB18	*DG5*		*4/5*	*268.9*	*−70.8*	*4145.9*	*1.4*		*17.927*	*73.714*
MB29		972	6/7	163.9	25.9	56.4	9.0	10.01	17.928	73.631
MB30		953	8/8	141.8	59.5	158.1	4.4	8.69	17.929	73.633
				Ambenali Formation						
MB20		940	9/9	141.1	59.1	113.8	4.9	9.57	17.929	73.634
MB14		911	8/8	128.1	57.3	44.2	9.4	17.59	17.935	73.633
MB30–MB14	*DG4*		*3/3*	*136.8*	*58.8*	*372.0*	*6.4*		*17.931*	*73.633*
MB13		898	7/7	91.1	66.0	59.4	9.1	22.88	17.934	73.633
MB16		845	11/11	144.8	45.1	225.0	3.1	4.39	17.936	73.626
MB15		775	10/10	161.3	45.6	341.7	2.6	3.71	17.933	73.618
MB21		755	8/8	155.6	26.7	37.3	9.8	10.98	17.940	73.590
MB23		735	9/9	169.2	62.7	23.6	10.9	24.34	17.943	73.587
MB26		722	12/13	179.1	58.3	184.3	3.2	6.10	17.932	73.610
MB22		710	6/8	178.2	57.9	104.5	6.7	12.68	17.946	73.586
MB23–MB22	*DG3*		*2/3*	*178.7*	*58.1*		*σ = 7.4°*[b]		*17.940*	*73.594*
PA01		650	9/9	130.6	39.6	82.1	5.8	7.53	17.943	73.572
PA02		638	7/7	139.8	35.9	4.3	34.1	43.79	17.942	73.571
PA03		583	9/9	174.6	43.6	201.0	3.6	4.97	17.936	73.566
PA10		563	7/9	142.1	52.6	200.7	4.6	7.58	17.933	73.562
PA11		555	6/9	163.3	65.7	48.4	11.5	29.00	17.934	73.560
PA08		515	8/8	155.7	33.6	197.2	4.0	4.80	17.932	73.560
PA09		474	7/8	155.4	16.8	100.1	6.1	6.37	17.934	73.554
PA19		433	7/9	139.8	45.2	33.5	11.6	16.58	17.935	73.551
				Poladpur Formation						
PA18		356	8/8	152.8	56.2	62.4	7.1	12.83	17.933	73.549
PA17		310	9/9	169.8	52.9	349.1	2.8	4.64	17.934	73.543
PA16		290	8/8	151.0	53.0	103.5	5.8	9.67	17.934	73.541
PA15		255	8/8	181.5	54.5	210.1	3.8	6.54	17.935	73.537
PA18–PA15	*DG2*		*4/4*	*163.8*	*54.8*	*89.1*	*9.8*		*17.934*	*73.543*
PA07		187	8/8	138.6	51.0	55.3	9.0	14.39	17.936	73.525
PA06		149	7/7	149.7	27.1	30.3	11.3	12.71	17.938	73.523
PA05		121	7/9	148.7	52.8	35.4	9.5	15.84	17.938	73.518
PA07–PA05	*DG1*		*2/3*	*143.6*	*52.0*		*σ = 13.1°*[b]		*17.937*	*73.522*
PA04		107	10/10	165.4	38.1	195.2	3.5	4.45	17.939	73.515
PA14		96	8/8	31.6	77.4	837.9	1.9	8.74	17.971	73.490
PA13		65	9/9	91.3	54.2	33.3	9.3	16.03	17.975	73.482
PA12		22	9/9	151.3	37.2	270.4	3.1	3.89	17.977	73.470
Mean directions[c]										
Using site directions			29/44[d]	157.9	45.7	28.3	5.1		17.96	73.6
Using DG directions			17/44[d]	155.6	41.3	25.7	7.2		17.96	73.6

[a]MP, Mahabaleshwar-Poladpur; DG, directional group is group of statistically similar directions (see text); *n*/N, number of sites used in the statistics/number of sites; Dg,Ig, declination/inclination in geographic coordinates; κ and α_{95}, parameters of Fisher statistics; dDg, confidence limits of declination; Slat,Slon, latitude and longitude of sites.

[b]In the case of $n = 2$, α_{95} cannot be calculated and the value $\sigma = \sqrt{\Sigma (\alpha_{95\ 1}{}^2 + \alpha_{95\ 2}{}^2)}$ is listed (see text).

[c]Mean directions are given using the Fisher statistics.

[d]Number of sites used in calculating of the mean/total number of sites; directions with $\alpha_{95} > 10$ and transitional and excursional directions are removed.

characteristic primary direction. Complete demagnetization generally occurs between 540 and 580°C for most samples, except for nine sites MB08, MB10, MB16, MB18, MB19, MB23, PA01, PA03, and PA18 which have higher unblocking temperatures, probably due to the presence of minor (titano)hematite. This component always records the same direction as the main titanomagnetite component. Site-mean directions of these HTCs display two distinct but opposite

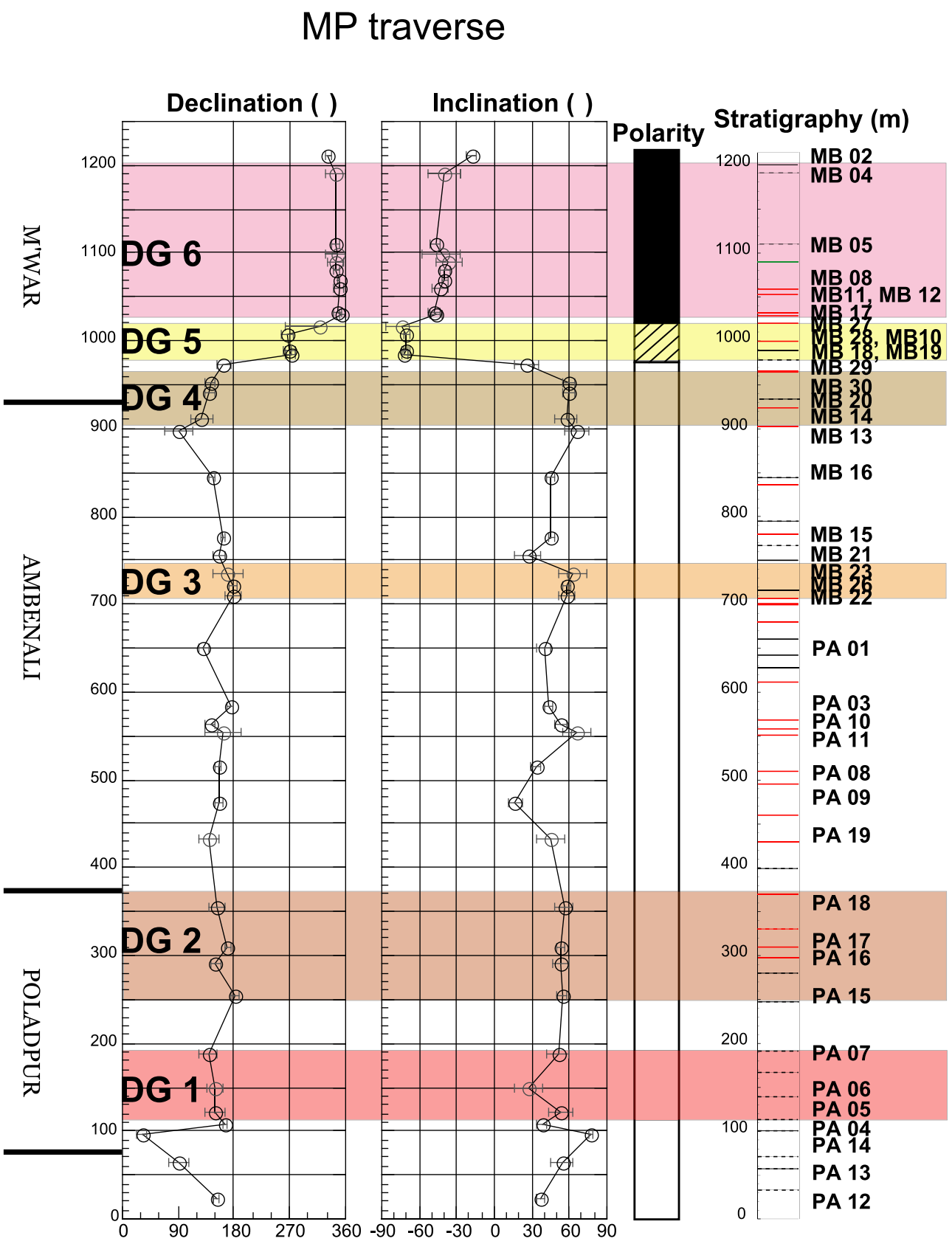

Figure 4. Magnetostratigraphic log of site mean directions (declination and inclination). Each well-preserved flow is defined by contact between two successive flows (black lines) and the presence of red/green boles (red/green lines) [*Jay*, 2005]. In the case of absence of secular variation, we define directional groups, which correspond to major single eruptive events (see text; site polarities: black, normal; white, reversed; hatched, transitional).

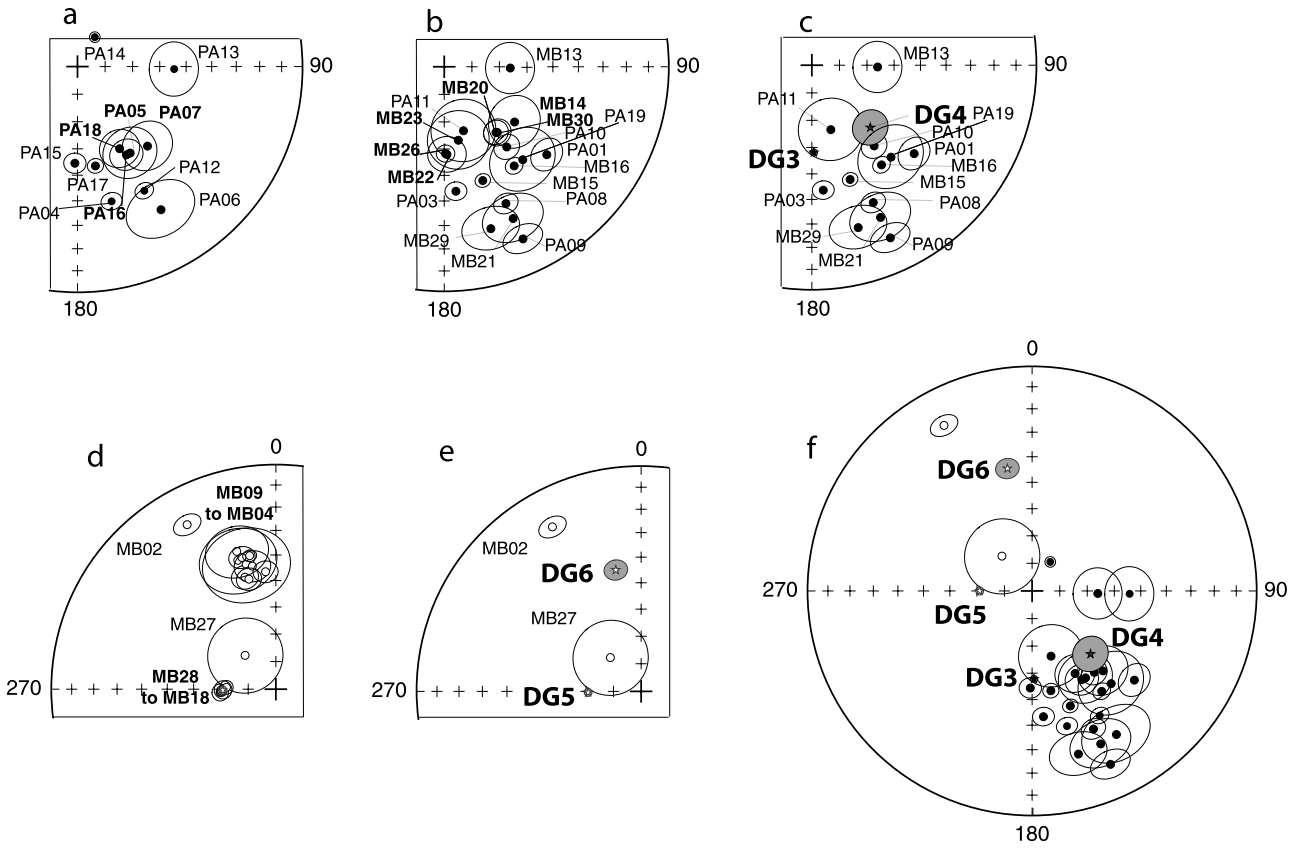

Figure 5. Equal-area (stereographic) projections of site mean directions for the M'war-Poladpur section. (a) Lower third of the section from site PA12 at bottom to PA18 at top. Note some possibly excursional directions (PA13 and PA14) and similar directions (PA05-PA07, PA16-PA18 in bold) corresponding to possible directional groups (DG1?, DG2?) though reasons to doubt the reality of these are given in text. (b) Middle part of the section from site PA19 to the top of the reversed zone at MB29. A number of directions marked in bold correspond to directional groups DG3 and DG4. (c) Same as Figure 5b but with DGs replacing their individual site means, i.e., independent cooling units only are shown. (d) Top part of the section, from MB18 to MB02, with the transitional and normal parts. Directions marked in bold correspond to directional groups DG5 and DG6. (e) Same as Figure 5d but with DGs replacing their individual site means, i.e., independent cooling units only are shown. (f) Summary of directions for the whole section with only independent volcanic (cooling) units shown.

polarities, in agreement with previous magnetic studies [*Kono et al.*, 1972; *Vandamme et al.*, 1991; *Khadri et al.*, 1999]. The 30 lowermost sites (up to 972 m) representing the Poladpur and Ambenali formations as well as the lowest flows of the M'war Formation, have reversed polarity. The 10 uppermost sites (from 1030 to 1210 m) have normal polarity. The five mean directions for flows located between the above mentioned lower and upper parts of the section (985 – 1007 m) have very similar and high inclination values. These transitional lava units were emplaced during a polarity reversal.

[30] The magnetic polarity stratigraphy (Figure 4) is consistent with earlier reports on the Mahabaleshwar sections, from the early work of *Kono et al.* [1972], who located the reversal at 940 m, to *Jay* [2005], who located it at 964 m. Our detailed sampling of the transitional flows places them between 980 and 1007 m. Part of these differences may be due to differences in focus to identify all transitional flows, part to the limited precision of the different altimeters and GPS instruments used in the more recent surveys.

3.2. Directional Groups in the M'war-Poladpur Section

[31] We have analyzed paleomagnetic directions of successive lava units, in order to check whether they could be considered as being statistically identical, using a test modified from *McFadden and McElhinny*'s [1990] reversal test [*Cogné*, 2003]. *Mankinen et al.* [1985] recognized that thick lava sequences which have recorded the same paleomagnetic direction (in a statistical sense) likely were emplaced by eruption(s) which did not extend over sufficient time to record secular variation (SV). This has recently been applied to the cases of the Greenland traps [*Riisager et al.*, 2002, 2003a, 2003b, 2005] and central Atlantic magmatic province [*Knight et al.*, 2004; *Nomade et al.*, 2007; *Verati et al.*, 2007]. A statistically homogeneous paleomagnetic direction found in successive lava units defines a directional group (DG). Each DG is thus a robust indication of rapid emplacement of a (possibly very large) single eruptive event (SEE), implying very short eruptive climaxes.

[32] The duration required to record significant secular variation can be estimated based on behavior of the Earth's

magnetic field in the historical past, and assuming that characteristics of SV remained similar in the past hundred millions years. In the past 4 centuries, the geomagnetic field direction in Europe has shifted by as much as 15° (10° in inclination and 25° in declination [*Gallet et al.*, 2002]). In the past 3000 years, the field in Europe has followed irregular loops of up to 20° amplitude, on characteristic time constants on the order of 500 to 1000 years, with a number of standstills and hairpins, and a number of faster track segments [*Gallet et al.*, 2002; *Genevey and Gallet*, 2002]. We have calculated the distribution of along-track secular variation (SV) velocities for that time period, which we find to have lognormal shape with a strong mode at about 2°/100 years. For older, geological periods, the amplitude of paleosecular variation is fairly well constrained, but not its velocity (see discussion by *Merrill et al.* [1996]). The characteristics of recent secular variation can be used to estimate whether magnetic directions of successive Deccan lava units are separated by more or less than, say, a century: successive flows with directions differing by less than a few degrees could have been emplaced in a short time of decades. Of course, sources of differences between the mean directions also include intraflow variance. This is translated into the α_{95} confidence interval of each mean. One can therefore test whether the difference between two successive directions is statistically significant. The mean α_{95} of our site mean directions is on the order of 4°, consistent with the idea that statistically identical directions could differ in time by no more than a couple hundred years. A potential (nonuniqueness) problem arises from the fact that secular variation loops may cross, and that two identical directions could be separated by the time taken for a full SV loop to be completed. But statistically identical directions in flows directly overlying each other stand a large probability of having been recorded in a short time (the measuring stick being the modal SV rate of ~2°/100 years).

[33] A simple method has been developed in order to detect the occurrence of directional groups (DGs) and to define precisely which lava units belong to a given DG. This method is given in the auxiliary material.[1] Going from bottom to top of the section (Table 1 and Figures 4 and 5), we have thus been able to identify four clear directional groups (labeled DG3, DG4, DG5, DG6) and two more uncertain ones (DG1, DG2). The series starts with four flows with distinct magnetic directions (PA12, 13, 14 and 04), which have recorded (large) secular variation within the same reversed chron. Continuing upward, we find that site mean directions for PA05 and PA07, separated by at least 60 m, are statistically identical ($\delta = 6.4° < \sigma = 13.1°$) (Figure 5a). This would lead us to propose a first directional group (DG1). However, intervening site PA06 has been excluded, because its α_{95} is above the threshold of 10°. Yet, this ill-defined direction appears to be distinct from those of PA05 and PA07, weakening the significance of DG1. Site PA15 (255 m) has a well-defined direction, distinct from PA07 of DG1, implying that some secular variation had time to take place between the two. Our test shows that sites PA16 and 18 have statistically identical directions (Figure 5a), which could indicate a second DG (DG2). But intervening site PA17 cannot be included in that group. Its confidence interval does not intersect the confidence intervals of either direction from the flows above or below. Moreover, new K-Ar dating [*Chenet et al.*, 2007] assigns PA17 an age of 62.0 ± 0.6 Ma, which is clearly distinct (younger by a couple Ma) from other ages along Poladpur-M'war section. The lava unit in which PA17 was sampled could be a sill. Thus PA17 cannot be included in DG2 and weakens the significance of that group. It remains awkward and noteworthy that four nearby but not successive, independent flows sampled four times the same paleomagnetic direction.

[34] A sequence of five flows with distinct site-mean directions (PA09, 08, 10, 03 and 01; PA11 is disregarded because α_{95} is >10°) follows. Sites MB22 and 26 (MB23 has α_{95} just above cutoff, but is compatible) form a third directional group DG3 (Figures 5b and 5c). The magnetic directions of MB22 and MB26 are very close (δ= 0.6°, σ = 7.4°). Adding flows above or below drastically increases σ and the SEE cannot be extended further. DG3 is followed by four discrete, independent directions MB21, 15, 16, and 13. MB13 could be an excursional direction.

[35] The rest of the lava unit succession is particularly interesting, as it appears to comprise three distinct DGs. Our test shows that MB14, 20, and 30 form reversed DG4, with α_{95} = 6.4° (Figures 5b and 5c). Attempting to add flow MB13 below or MB29 above fails the SEE test. MB18, MB19, MB10, as well as MB28 (MB27 has α_{95} above cutoff, but is compatible) form the very tightly grouped transitional DG5, with α_{95} = 1.4° (Figures 5d and 5e). Finally, the upper part of the section is made of nine lava units (MB09, 17, 12, 11, 08, 05; MB07, 06 and 04 are compatible but excluded from computation of the overall mean because of α_{95} above cutoff) which form the thick DG6, with α_{95} = 3.9° (Figures 5d and 5e). Only sites MB29 (between DG4 and DG5) and MB02 (the topmost site) have directions not belonging to these groups in the 300-m-thick lava pile between altitudes of 900 and 1200 m.

[36] We note that the two thickest red boles occur between distinct magnetic directions (MB29-MB30 and MB22-PA01). But thinner red boles are sometimes located at contacts between lava flow units within a flow field (or SEE), which has important implications for the duration of their formation.

[37] In addition to paleomagnetism, we have tested the existence of chemical correlation within the sections. This correlation is based on the degree of similarity, which is represented by a statistical value defined as a Euclidean distance D between two samples:

$$D^2 = \sum_{k=1}^{n} \left[\frac{\left(x_a^k - x_b^k\right)^2}{2\sigma_k^2} \right]$$

where $x_a^k (x_b^k)$ is the concentration of element k in lava unit a (b), σ_k is the standard deviation for analytical precision of element k, n is the number of elements. This approach has been proposed by *Perkins et al.* [1995] and applied by *Jay* [2005] to lavas sampled in a single sheet lobe of the M'war section. The statistical distance D^2 follows a χ^2

[1] Auxiliary materials are available in the HTML. doi:10.1029/2006JB004635.

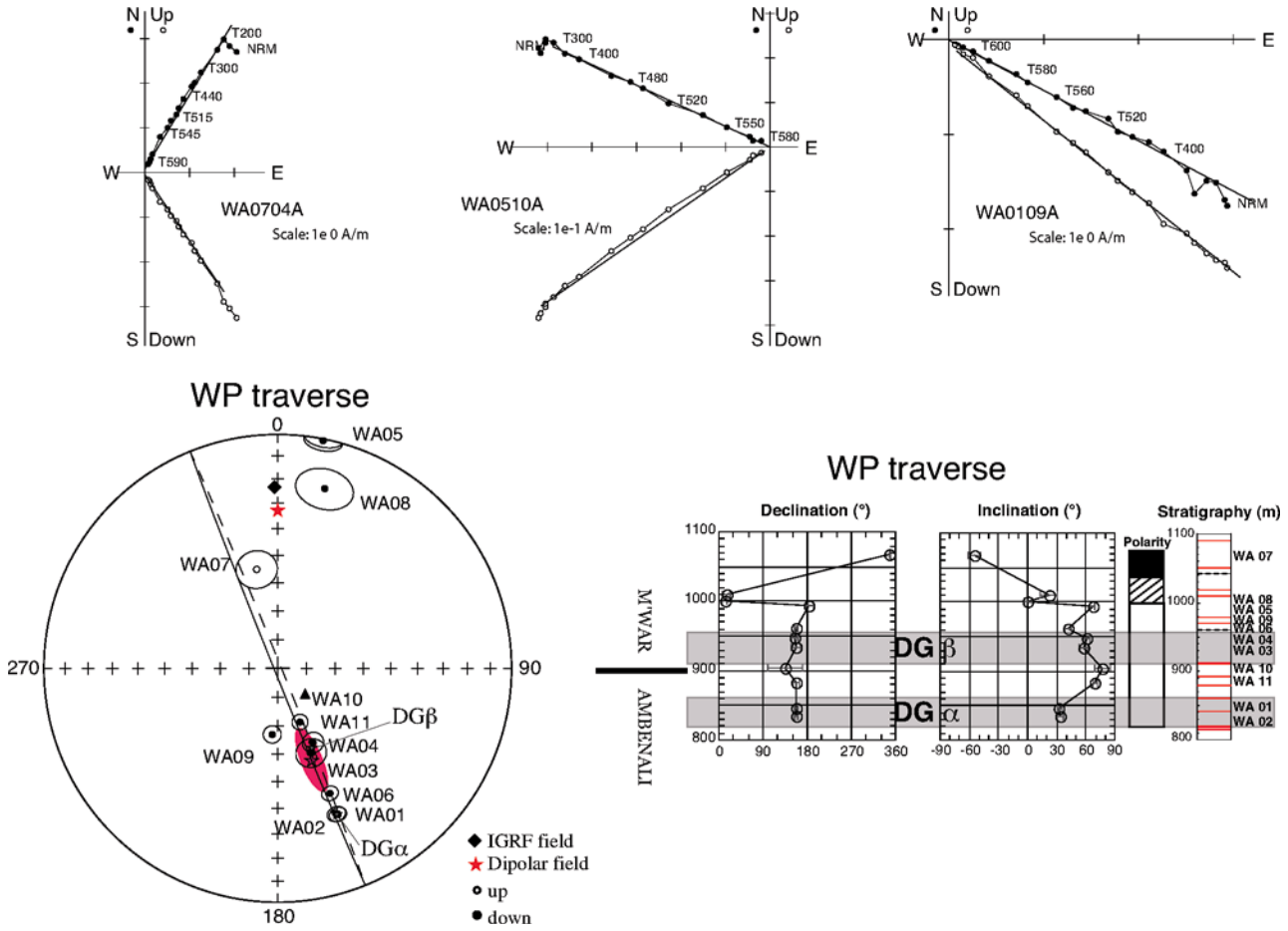

Figure 6. Summary of results for the companion Wai-Panchgani section. (a) typical results from thermal demagnetization of three samples. (b) Equal-area (stereographic) projections of site mean directions (stars indicate the mean directions of DG) with Fisherian and bivariate means, IGRF and dipole field directions indicated. Black triangle represents mean direction of site WA10 calculated using only two samples for which α_{95} cannot be calculated. (c) Magnetostratigraphic log of site mean directions and indication of DGs as in Figure 4.

distribution with n degrees of freedom. The larger the Euclidean distance D^2, the lower the probability of similarity (i.e., correlation). We have determined in this way the degree of similarity of successive lava units along the 1200-m-thick MP section based on the concentrations of 22 elements (notably rare earth elements) out of 41 measured, 19 elements having too small a concentration, or a concentration close to the standard deviation, or being known to be mobile (such as Ba). The largest degree of similarity (confidence level >95%) is always found within directional groups, suggesting that successive lava units composing a directional group were emplaced during a single eruptive event from a single source. However, the opposite may also occur. Two lava units belonging to a given magnetic directional group can be chemically distinct. Such is the case for MB11 and MB08 in DG6 (angular distance = 2.6° but confidence level of chemical similarity ~15%). This may suggest two distinct eruptive events (from distinct chemical sources) over a period short enough not to have recorded secular variation.

3.3. Paleomagnetic Results for the Wai-Panchgani Ghat Section

[38] In order to test the paleomagnetic results from the main section, we have also determined the magnetostratigraphy of the Wai-Panchgani (WP) road section (Figures 1a, right, and 1b). This should allow better constraints on the lateral extent of the lava units. Demagnetization results closely follow those discussed above, with LTC close to the recent magnetic field and a generally well-isolated HTC (Figure 6a). The unblocking temperatures occur between 540 and 580°C. The bottom of the Wai section has reverse polarity (sites WA02 to 09), whereas the top of the traverse is normal (site WA07). Sites WA08 and 05, with a clear transitional polarity, testify to emplacement of two lava flows during the magnetic reversal. So, volcanic activity was taking place during the ~5000 years of the reversal event at both sections, although our sites are not from the same flow field, magnetic directions being statistically distinct.

[39] Comparing the detailed directions of successive lava flow units (as a function of their α_{95} confidence intervals),

Table 2. Paleomagnetic Results for the Wai-Panchgani Ghat Section[a]

Site	DG	Altitude (m)	*n*/N	Dg (deg)	Ig (deg)	κ	α_{95} (deg)	dDg	Slat (deg)	Slon (deg)	α_{95} x	α_{95} y	Ratio	Azimuth
						Mahabaleshwar Formation								
WA07		1067	6/8	348.0	−54.4	96.5	6.9	11.91	17.932	73.830				
WA08		1010	6/10	14.6	21.7	73.5	8.4	9.04	17.929	73.838				
WA05		1000	14/15	11.3	0.8	69.3	4.8	4.80	17.929	73.839				
WA09		994	9/9	184.7	66.9	286.9	3.0	7.67	17.931	73.842				
WA06		961	*10*/10	157.3	41.6	323.4	2.7	3.61	17.932	73.844				
WA04		948	9/9	154.5	61.2	204.8	3.6	7.49	17.932	73.846				
WA03		935	4/8	158.4	58	319.4	5.1	9.65	17.932	73.848				
WA03–WA04	*DGα*		*2/2*	*156.6*	*59.7*		*σ = 6.2*[o b]		*17.932*	*73.847*				
						Ambenali Formation								
WA10		903	2/3	135.1	76.8		σ = 5.7[o b]	35.4	17.934	73.853				
WA11		883	8/9	157.5	69.8	411.8	2.7	7.84	17.935	73.855				
WA01		846	12/12	157.6	32.9	264.9	2.7	3.21	17.939	73.859				
WA02		834	10/10	158.0	33.3	285.5	2.9	3.47	17.940	73.86				
WA01–WA02	*DGβ*		*2/2*	*157.8*	*33.1*		*σ = 4.0*[o b]		*17.940*	*73.860*				
Mean directions[c]			9/11[d]	159.8	55.5	3.5	12.5	22.46	17.933	73.847	3.5	12.5	3.6	157.5
Wai section with			7/11[d]	160.7	58.2	4.4	13.7	26.70	17.932	73.845	4.4	13.7	3.1	160.1
Wai section with DG														

[a]WP, Wai-Panchgani; DG, directional group: group of similar directions (see text); *n*/N, number of sites used in the statistics/number of sites; Dg,Ig, declination/inclination in geographic coordinates; κ and α_{95}, parameters of Fisher statistics; dDg, confidence limits of declination; Slat, Slon, latitude and longitude of sites; α_{95}x, α_{95}y, semiaxes of the bivariate ellipse of 95% confidence; Ratio, elongation of the bivariate ellipse of 95% confidence (α_{95}x/α_{95}y); Azimuth, azimuth of the main axis of the bivariate ellipse of 95% confidence.

[b]In the case of $n = 2$ sites, α_{95} cannot be calculated and the value $\sigma = \sqrt{(\alpha_{95\ 1}{}^2 + \alpha_{95\ 2}{}^2)}$ is listed (see text).

[c]Mean directions are given using the Bivariate statistics.

[d]Number of sites used in calculating the mean/total number of sites; directions with $\alpha_{95} > 10$ and transitional and excursional directions are removed.

we identify two directional groups, which could have recorded the same paleomagnetic direction within a few degrees: sites WA01 and 02 forming DGα, and sites WA03 and 04 forming DGβ (Figures 6b and 6c). Sites WA10 and 11 have only marginally intersecting confidence intervals, which we therefore do not interpret as a third group (there are only few available samples from WA10, due to strong weathering of the exposure) (Table 2). In the field, site WA06 appeared to belong to the same flow field as sites WA03 and 04 (lack of visible discontinuity) but has not recorded the same direction. This could imply that there is an unseen contact (due to weathering and vegetation) between two separate flows in this part of the section (or that we have failed to separate a component of remagnetization in some of the flows, see below).

[40] But the most conspicuous feature observed in the WP section and not in the MP section is that almost all site means except for the two transitional flows (WA05 and 08) and the immediately underlying flow WA09, are aligned along a well-defined great circle (Figure 6b): this circle is not far from the one that can be drawn between the average reversed primary direction of the other section and the recent (or dipole) field. It is even closer, actually identical to the circle that passes through the primary direction and the vertical (both circles of course include also the normal primary direction). The distribution is not Fisherian, and the bivariate mean is given in Table 3. It so happens that the mean of the WP section reversed directions is very similar to that of the MP section, but the uncertainty is a very elongated ellipse with a major to minor axis ratio of 3.6. We may have been unable to separate the HTC from an overprint, which would behave in almost the same way as the primary component upon demagnetization. This overprint could be linked to the terminal phases of volcanism, which have normal polarity, not far from the top of the series, its capping laterite, and a well watered low-slope watershed. The potential partial (and largely hidden) remagnetization of sites from the WP section is not strong enough to prevent us from unambiguously identifying magnetic polarities, two ~40- to ~50-m-thick directional groups of reversed polarity (DGα, DGβ) and a ~35-m-thick set of two transitional flows. On the other hand, remagnetization

Table 3. Mean Directions of the Upper Formations of the Western Ghats[a]

Formation	Statistics	*n*/N	Dg (deg)	Ig (deg)	κ	α_{95} (deg)	α_{95}x	α_{95}y	Ratio	Azimuth	Slat (deg)	Slon (deg)	Reference
MP ghat section	Fisher	29/44[b]	157.9	45.7	28.3	5.1					17.9	73.6	this study
MP ghat section with DG	Fisher	17/44	155.6	41.3	25.7	7.2							this study
WP ghat section	Bivariate	9/11	159.8	55.5			3.5	12.5	3.6	157.5	17.9	73.8	this study
WP ghat section with DG	Bivariate	7/11	160.7	58.2			4.4	13.7	3.1	160.1			this study
Combined mean direction		24	156.7	46.2	21.1	6.6					17.9	73.65	this study
Mahabaleshwar		28	160.5	46.8	15.6	6.7					17.92	73.58	*Kono et al.* [1972]

[a]Parameters are *n*/N, number of sites used in the statistics/number of sites; Dg, Ig, declination/inclination in geographic coordinates; κ and α_{95}, parameters of Fisher statistics; α_{95}x, α_{95}y, semiaxes of the bivariate ellipse of 95% confidence; Ratio, elongation of the bivariate ellipse of 95% confidence (α_{95}x/α_{95}y); Azimuth, azimuth of the main axis of the bivariate ellipse of 95% confidence; Slat,Slon, latitude and longitude of sites. Italics indicate the directional groups.

[b]Number of sites used in calculating the mean/total number of sites; directions with $\alpha_{95} > 10$ and transitional and excursional directions are removed.

may have displaced HTC directions and blurred the picture, which could have allowed us to identify identical directions between the two sections. Samples from the WP section are the subject of further ongoing analyses, particularly of magnetic anisotropy. Our paleomagnetic analyses confirm field observations indicating that the eastern side of the Mahabaleshwar plateau is more altered than the western side. The number of thick red boles is more important than in the companion section. Intense and continued weathering from the Cenozoic up to the Present due to the Indian monsoon has considerably altered the flows and erased many lava outcrops on the eastward facing watershed, in contrast to the western escarpment which is constantly refreshed by erosion.

3.4. Correlations Between the Two Sections

[41] Comparisons between magnetic directions of lava units respectively belonging to the MP and WP sections (Figure 7), which are separated by some 20 km and have recorded the same simple R-T-N polarity sequence, may allow us to constrain the lateral extent of flows and cooling units, and therefore the sizes of these volcanic units, as is further discussed in section 4.2. Paleomagnetic characteristics are almost identical and allow some fine correlation, when stratigraphic thicknesses can be quite different. DGs, which are considered as evidence of single events erupted over a short time interval, possibly as short as a century or even less, are particularly useful potential correlation tools.

[42] As a first example, the direction found in the single lava unit sampled in the Ambenali Formation at MB21 in the MP section is found again as DGα in the WP section, formed of the two lava units WA01 and 02, also in the Ambenali Formation. We infer that the same sheet lobe has been sampled at both locations over 20 km apart: the thickness of that sheet lobe changes from 28 m in the MP section to 40 m in the WP section.

[43] Lava units, which have recorded the C29R-C29N magnetic transition, are located between 980–1020 m in the MP section and 980–1010 m in the WP section, but they display different magnetic directions. This implies that regional volcanic activity continued over some time (thousand year scale), though transitional flows encountered in both sections are not from a single lava unit. Transitional flow thickness varies from 30 m in WP (three lava units bounded by two red boles) to 40 m in MP (also three flows, two red boles and one direct contact).

[44] Above the transitional directions, the lava units with normal polarity are DG6 and WA07 respectively. Although the two directions are not the same, they are relatively close and a small amount of undetected normal overprint in WA07 would bring it in coincidence with DG6. Thicknesses cannot be compared there because some of the uppermost flows of the M'war Formation could not be sampled in the WP section due to extensive weathering. For this reason, the M'war Formation appears to be thicker in the WP section ($\sim$175 m) compared to the MP section ($\sim$130 m).

[45] Altogether, we can build a case for a reasonable correlation (for three flow packages) between the two sections for the top of the Ambenali and the lower Mahabaleshwar Formations, from 750 to above 1050 m in the MP section (=300 m thickness), and 810 to 1070 m in the WP section (=260 m thickness). The difference ($\sim$40 m) in the thicknesses between the two sections is 15% and can be attributed to either flow base topography or differences in lava unit thickness or both. Such differences imply differential slopes of 50 m over 20 km, or less than 3×10^{-3}, which is undetectable in the field without careful altitude measurements, as previously pointed out by *Courtillot et al.* [1986] and *Vandamme et al.* [1991]. Comparing lava thicknesses in different traverses around the Mahabaleshwar plateau (based mainly on geochemistry, with help from the reversal boundary as a singular marker), *Jay* [2005] indicated that thickness of the Mahabaleshwar Formation was thicker over the Ambenali Ghat area (i.e., MP section) than in other sections of the Mahabaleshwar Plateau (such as the WP section). This may be due to the fact that a topographic high in the lava pile developed in this area prior to Mahabaleshwar emplacement. Chemical correlation was also used to correlate lava units of the two sampled sections. Unfortunately, the chemical variability (for the 22 selected REE) along the section is strong and does not allow to correlate lava units between the MP and WP sections, or even within the WP section itself. This agrees with *Jay*'s [2005] conclusions; however, paleomagnetic results show that directional correlations can be more diagnostic than chemical ones.

3.5. Paleomagnetic Mean Directions and Poles

[46] The overall (Fisherian) mean direction for the MP section is D = 157.9°, I = 45.7° (N = 29, α_{95} = 5.1°, κ = 28.3), when all flows are taken as units, and D = 155.6°, I = 41.3° (N = 17, α_{95} = 7.2°, κ = 25.7), when directional groups (considered to be individual, independent single eruptive events; Table 3) are used. Note that transitional and excursional flows are not included in computation of the mean. For the WP section, we have seen that data points were well defined but did not form a Fisherian distribution. The bivariate mean direction is D = 159.8°, I = 55.5° (N = 9, α_{95x} = 3.5°, α_{95y} = 12.5°), when all flows are taken as units, and D = 160.7°, I = 58.2° (N = 7, α_{95x} = 4.4°, α_{95y} = 13.7°), when directional groups are used (Table 3). The combined mean for all directional groups and individual flows from the two sections, excluding transitional directions, lies at D = 156.7°, I = 46.2° (N = 24, α_{95} = 6.6°, κ = 21.1). But we do not retain it as the best value to be added to the global database, because of the non-Fisherian distribution of the site means of the WP section. So the MP section mean direction (based on directional groups or single lava units) is our preferred value for the Mahabaleshwar plateau formations. This direction is quite similar to the mean direction obtained by *Kono et al.* [1972], almost 35 years ago: D = 160.5°, I = 46.8° (N = 28, α_{95} = 6.7°). This testifies to the quality of that early work, despite a methodology which would now be considered insufficient for inclusion of the data in a reliable global database.

[47] The distribution of some virtual geomagnetic poles (VGP) is displayed in Figure 8. The MP mean pole lies at λ = 42.0°N, ϕ = 284.2°E (N = 17, dp = 5.3°, dm = 8.7°); the WP pole distribution is strongly non-Fisherian as outlined above and is therefore not considered further. In this calculation, directional groups are counted as only one [e.g., *Riisager et al.*, 2003a, 2003b], in order to avoid overrepresentation of the same instantaneous photograph of the Earth's

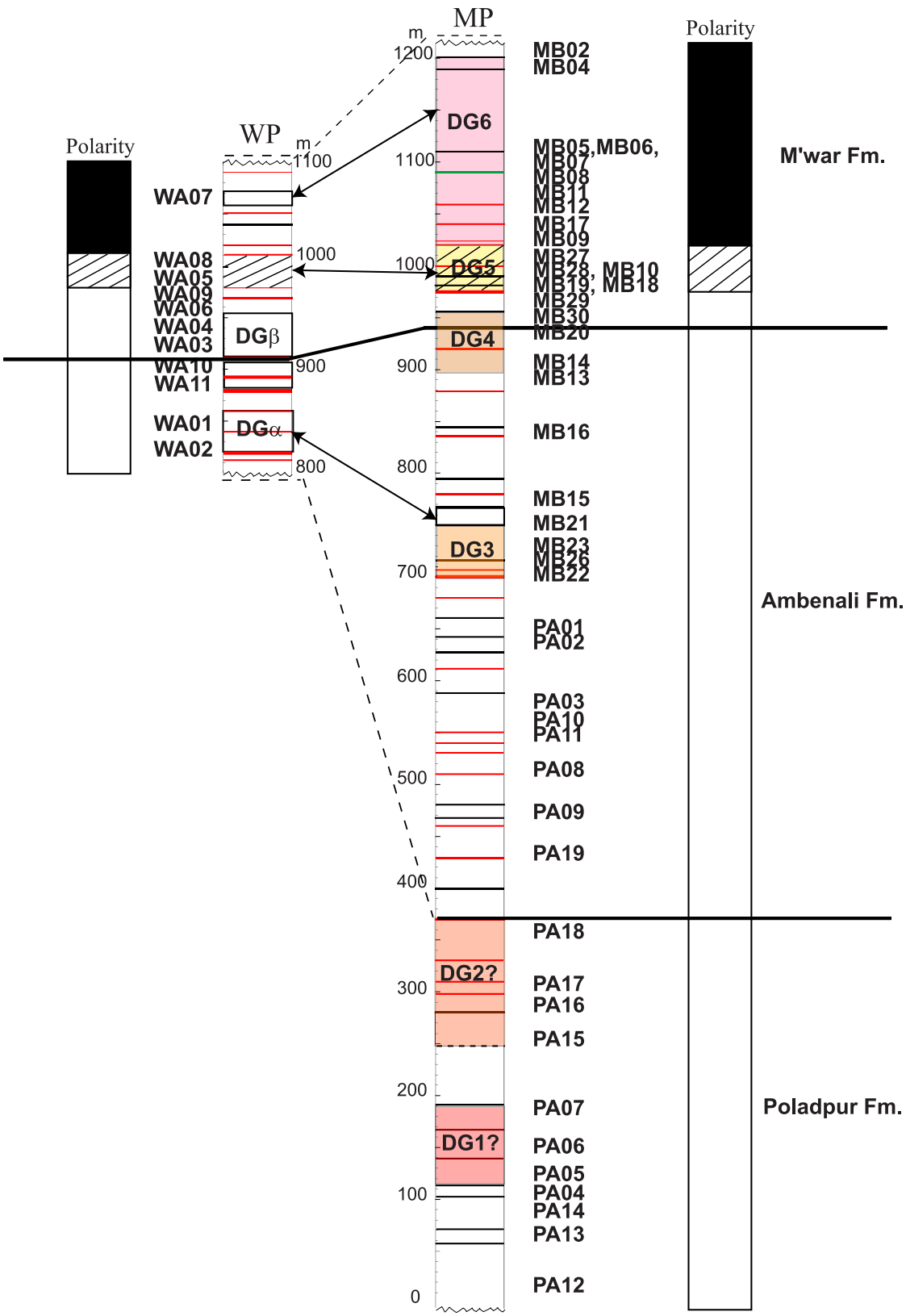

Figure 7. Correlations between the two sections with flow boundaries, red boles, magnetic polarity, and directional groups indicated (see text).

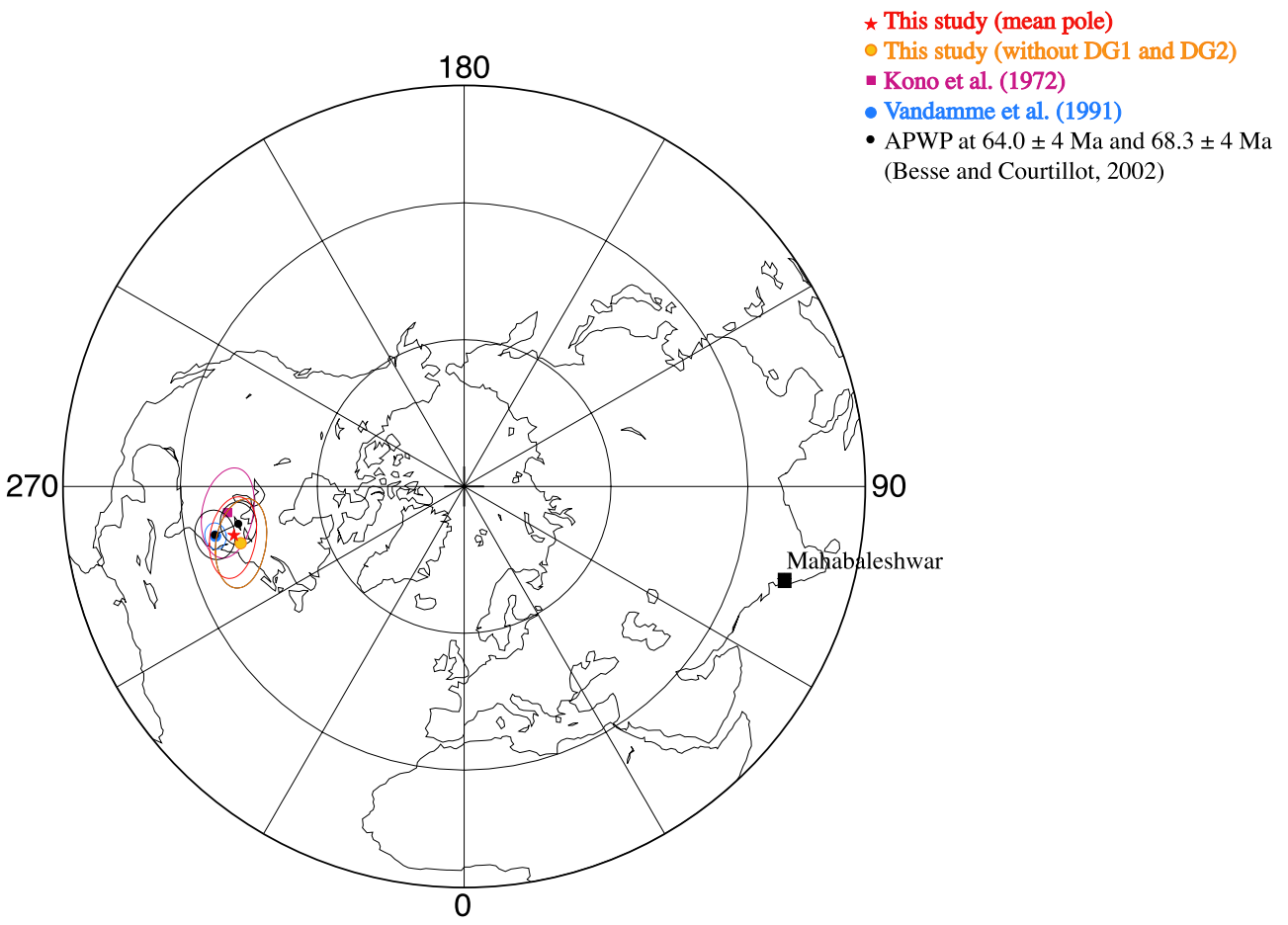

Figure 8. Equal-area projections on the Northern Hemisphere of paleomagnetic poles. The red star corresponds to our mean VGP, the orange circle corresponds to the same but without suspect DG1 and DG2, the blue circle corresponds to the mean pole calculated by *Vandamme et al.* [1991] along a Nagpur-Bombay traverse, and the purple circle corresponds to the pole of *Kono et al.* [1972]. Also indicated are a couple of 64 and 68 Ma poles from the synthetic apparent polar wander path for India from *Besse and Courtillot* [2002].

field, and transitional and excursional directions are removed (sites MB28-18, MB13, PA13, PA14).

[48] This is to be compared for instance to *Kono et al.*'s [1972] pole for the same region (which lies at $\lambda = 40.3°$N, $\phi = 276.3°$E, dp = 5.6°, dm = 8.6°, N = 28 sites; note that in the original paper the pole is apparently erroneously calculated at $\lambda = 38.3°$N, $\phi = 263.3°$E with $A_{95} = 7.4°$), or to the grand average pole for the whole Deccan from the most recent, comprehensive review of Deccan trap poles, which lies at $\lambda = 36.9°$N, $\phi = 281.3°$E with $A_{95} = 2.4°$ (N = 163 sites) [*Vandamme*, 1990; *Vandamme et al.*, 1991]. We find that our new pole, based on a much smaller sampling,

Table 4. Compilation of Virtual Geomagnetic Poles Obtained for the Mahabaleshwar Plateau[a]

Section	*n*	Plat (°N)	Plon (°E)	A_{95} (deg)	κ	dp	dm	ASD	Statistic	Reference
MP ghat section	29	279.0	39.2	5.2	27.8			15.4	Fisher[b]	this study
	29	279.6	40.1			4.1	6.5		Fisher[c]	this study
MP ghat section with DG	17	283.5	41.1	6.7	29.0			15.1	Fisher[b]	this study
	17	284.2	42.0			5.3	8.7		Fisher[c]	this study
Mahabaleshwar	28	40.3	276.3	8.6	5.6					*Kono et al.* [1972]
Mahabaleshwar	46	39.2	277.9	4.9	19.6			18.4		*Vandamme et al.* [1991]
Deccan trap	163	36.9	281.3	2.4	21.6			17.4		*Vandamme et al.* [1991]
Nagpur traverse	16	38.4	282.4	6.1	37.9			13.2		*Vandamme et al.* [1991]
Mahabaleshwar	28	40	276	7.87	7.4					*Besse and Courtillot* [2002]
Deccan Traps	21	32.6	290.8	3.8	5.9					*Besse and Courtillot* [2002]
APWP at 68 Ma	15	36.8	281.0	4.5	74.5					*Besse and Courtillot* [2002]

[a]Parameters are *n*, number of sites; Plat, Plon, latitude and longitude of poles; dp/dm, half angles of the ellipse of confidence; A_{95}, radius of 95% cone of confidence; ASD, angular standard deviation.
[b]Fisher statistics on VGPs calculated from individual site directions.
[c]VGP calculated from Fisher mean of site directions.

both in terms of number of sites and extension of the sampled area, is fully compatible with both the grand average and *Kono et al.*'s [1972] poles (Figure 8 and Table 4).

[49] VGP scatter for our sections is 15.1°. This value is significantly larger than that predicted by *McFadden et al.* [1991] for that time and latitude (11.3° ± 1.6°), but is close to the value of angular standard deviation found by *Vandamme et al.* [1991] (17.4° ± 1.4°), calculated using a bootstrap method and based on a very large amount of Deccan data. For this reason, this value might be a better estimate of PSV at 65 Ma for the latitude range 20–30° than the one assumed by *McFadden et al.* [1991]. Otherwise, there would be a large (~11°) additional, independent source of scatter, the same in all studies of the Deccan and confirmed by our new study (which meets generally accepted selection criteria for the paleomagnetic database). Should the latter interpretation be valid, the source of the additional scatter remains unclear.

[50] VGP distribution for the MP section shows no evidence of streaking that would indicate recording of the fast northward drift of India. Indeed, our new estimates of time and duration of volcanism (see section 4) further strengthen the view that not enough time was available in these upper Deccan formations to record any significant drift (for further discussion we refer the reader to *Vandamme et al.* [1991] extensive discussion, which remains largely valid).

4. Discussion, Implications, and Conclusions

4.1. Timing of Emplacement of the Upper Formations

[51] One of the main goals of the present study was to try to evaluate the total duration and time sequence of emplacement of the volcanic pile, i.e., the 49 successive lava units in the MP section and 15 in the WP section, as defined by *Jay* [2005]. Considerations based on physical volcanology of the Roza flow field in the Columbia River CFB have led *Thordarson and Self* [1998] to propose an upper limit on the total amount of time corresponding to active lava effusion. The four single lava units comprising the Roza flow field are estimated to have erupted in as short a time as a few months up to 5 years each. For the whole flow field, total eruption time is estimated between 5 and 20 years. The ranges are therefore roughly 1 to 10 years for single lava units. As a result, it is possible that the 1200-m-thick Poladpur section erupted in no more than (46 sampled lava units + 3 unsampled units) × (less than 10 years of emplacement time per cooling unit), i.e., roughly 500 years, and possibly less. These remarkably short values need independent confirmation.

[52] Analysis of paleomagnetic directional groups can provide particularly relevant evidence for such short durations: groups of successive lava units, which might have been considered as separate events based on flow structure and patterns but have recorded the same paleomagnetic direction (in a statistical sense), must have been formed in very short times. Note that the constraint from magnetic DGs is independent from those based on physical volcanology and thermal modeling. We have calculated the angular distance D between each lava unit in a SEE (DG) and the mean direction of this SEE. The mean angular distance D is 3.4° (±2.1°) for DG3, DG4, DG5, and DG6. The mean value increases up to 4.3° (±3.6°) if DG1 and DG2 are taken into account. These mean angular distances D of about 3° are similar to the modal secular variation per hundred years during the past 3000 years (section 3.2). They are also similar to the average 95% confidence interval of individual paleomagnetic directions, hence the smallest angular values that can be resolved. On the basis of the hypothesis that the nature of historical secular variation does represent the typical behavior of secular variation in geological time, these values lead us to estimate that the total duration for a single directional group could be on the order of a century, but could actually be less than a few decades if these angular differences are not statistically significant (i.e., distinct from zero). This is in a number of cases an even stronger constraint than that based on physical volcanology: indeed, if a SEE is composed of N single lava units, the total eruption time of the SEE is taken to be (N × 10 years) plus the unknown time elapsed between single units, whereas with the DG approach it is estimated as being on the order of or less than 100 years, placing far more stringent upper limits on the time elapsed between emplacement of successive single units comprising the SEE.

[53] Volcanic SEEs and individual flows can be clearly distinguished from each other. The angular distance between individual flows that do not belong to directional groups ranges from 11° to more than 100°, in contrast with the angular distances between lava units within DGs. Hence, groups DG3 (3 flows, ~40 m), DG4 (3 flows, ~65 m), DG5 (3 flows, ~40 m) and DG6 (7 flows, ~180 m), even adding the more uncertain DG1? (three flows, ~80 m thick) and DG2? (five flows, ~120 m), could each have been emplaced in <100 years (the total number of flows in the six DGs being 24). If we take 100 years and 10 years as upper and lower limits of effusion time, the upper estimate of the total time of lava effusion becomes $(49 - 24) \times 10 + 6 \times 100 = 850$ years, and the lower one $(49 - 24) \times 1 + 6 \times 10 = 85$ years! This is consistent with, and in a way vindicates the order of magnitude based on physical volcanology, again by placing stronger constraints on the time between a number of single units.

[54] The next question is how much time would have elapsed between successive flow emplacements not constrained by DGs? The presence of red boles is suggestive of significant time between flow units. Thick RBs (two in MP and four in WP) are actually never observed within a DG. We recall (section 3.1) that the formation of intertrappean red altered layers is linked to either a hydrothermal deuteric alteration process overprinting a weak weathering stage or pools of water retention (in the case of the thin < 20 cm red boles) or a longer weathering stage (saprolite formation) prior to the hydrothermal deuteric process (in the case of the thick red boles). In the latter case, duration of formation is estimated to have ranged from 1 to 50 ka. This estimate is based on data obtained from paleosols developed on different volcanic deposits (lava or pyroclastics) under various climatic conditions, such as in Cameroon or the Azores [*Benedetti et al.*, 2003; *Gérard et al.*, 1999, 2007], as well as volcanic constraints on the emplacement of the lava [*Self et al.*, 2006]. This range of time is consistent with that found in the Columbia River Basalt Province [*Sheldon*, 2003]. Alteration is a function of chemistry and climate. In Cameroon (4–12 m annual rainfall, 0–29°C, i.e., extreme hydrolyzing and contrasted conditions), calculated weathering rates, based on water-rock ratios and water inputs, range

from 1 to 100 mm a^{-1}. Physical properties of the parent material are another important factor. On massive lava flows, subjected to 9 m of annual rainfall at 29°C, a 2- to 10-cm-thick soil forms within flow fractures in less than 100 years. On vesicular pyroclastics submitted to 3 m annual rainfall at 20°C, more than 35 cm of soil forms on saprolite within 1500 years. For less drastic conditions (Azores, 1.5–2.5 m annual rainfall, 14°C), 5–20 cm of soil was found to have formed on pyroclastic rocks within 1000–10,000 years. During the Late Maastrichtian, climate was still warm and semiarid over the trap area (0.3–0.5 m annual rainfall, 25–30°C, based on climate modeling, not taking into account perturbations due to volcanic sulfur [e.g., *Donnadieu et al.*, 2006]), and fresh basalt flows are now thought to be particularly efficient CO_2 sinks through alteration [*Dessert et al.*, 2001]. This would have allowed for strong and fast weathering of lava flows tops; the above durations of formation may therefore be overestimates for the Deccan case. On the basis of these considerations, the total amount of time recorded by alteration or sedimentary bole levels in the 1200-m-thick MP section would be at least (2 thick RB) × (1 ka) = 2 ka up to (2 thick RB) × (50 ka) = 100 ka.

[55] On the other hand, the duration of formation of red boles may in many cases have been much shorter than generally assumed, i.e., less than 10 years for the thinner RBs (linked to a simple deuteric process). Three such thin red boles are located within the top part of DG1, two in DG4, one in DG5 and two (plus the only observed green bole) in DG6. The reasoning based on lack of recording of paleosecular variation within these directional groups implies that none of these nine red (or green) bole levels could have been formed in more than a few decades. This is at odds with previous studies which considered all weathering horizons as markers of long volcanic quiescence; it has implications for the architecture of the Wai Formation, as will be seen in the next section. This is a strong, new and independent argument in favor of a rapid alteration process.

[56] We finally estimate coarse bounds on the total amount of time recorded in the section by both volcanics and intertrappean levels to be between 85 + 2000 = 2085 yrs and 850 + 100,000 = 100,850 yrs. Clearly, the duration of actual eruptions appears to be almost negligible compared to the time between flows, as recorded by alteration, and possibly completely unrecorded in a number of instances. Also, an uncertainty comes from the durations between flows in direct contact which have left no stratigraphic trace. Lack of correlation between successive magnetic directions implies that at least a few centuries (say >500 years) must have elapsed, adding yet another minimum of [(49 − 24) + 6 − 1] × 500 = 15,000 years to the total duration. The range of estimates then becomes 17,085 to 115,850 years, which we round up as 15 to 115 ka, given large remaining uncertainties. A comparison of these durations with independent estimates would be a welcome test to our hypotheses. The K-T boundary has been located within a marine intratrappean sedimentary layer bounded by two lava units in the Rahjamundry traps [e.g., *Vandamme et al.*, 1991] and dated: these lava units are considered to be an equivalent of the Wai Formation [*Knight et al.*, 2003]. Therefore, the K-T boundary (65 Ma) must be located in the lower part of the MP section. A second time marker is given by the C29R-C29N magnetic transition, dated at about 250 ka after the K-T boundary [*Cande and Kent*, 1995]. This would imply that emplacement of the Poladpur-M'war section took place over 200 to 300 ka. Of course, a few lava flow units were probably omitted during sampling because of bad exposure or strong weathering, and a few direct contacts and red boles may have been missed. Nevertheless our hypothesis used in estimating total emplacement time seems entirely reasonable. Of course, this value does not have much precision, and the main uncertainty comes from the duration of formation of the very few thick red boles, which may mark the only truly significant breaks in volcanism.

4.2. Volumes of Eruptive Events and Eruption Rates

[57] In order to estimate eruption rates, the volumes of single eruptive events (DGs) must be evaluated. On the basis of the structure of the whole Deccan Traps (Figure 2a) rather than individual lava flow structure as observed in the field with limited outcrops, we propose that volumes of eruptive events identified as DGs are directly proportional to their thicknesses. The DGs, which altogether represent about one half of the thickness, i.e., one third to one half of the volume of the 1200-m-thick MP section (Figure 8), or about one sixth of the whole volume outcropping in the 3600-m-thick Western Ghats, may have been produced in less than 1000 years, if we consider only active effusion time (section 4.1). Directional groups identified by paleomagnetism correspond to major effusive SEEs produced over very short durations. They tend to have a homogeneous composition, hence homogeneous mechanical properties and in particular resistance to erosion. We can propose that the thickest ones may result in the major cliffs or steps which have given the traps their name (Figure 9). The small number of very large steps may be a reflection of the small number of very large SEEs.

[58] Careful analysis of volcanic features has allowed *Jay* [2005] to describe the architecture of the MP section. *Jay* [2005, p. 20] defined a flow field, the largest erupted unit and the product of a single eruption or vent, as "an aggregate product of a single eruption, [...] built up of one or, usually, more lava flows", bounded by red horizons, which were all then considered as marking longish periods of volcanic quiescence. Analysis of paleomagnetic secular variation allows us to further identify single eruptive events, which can in some cases be even more voluminous than volcanologically defined flow fields. For instance, DG6, which is almost 200-m-thick, contains at least four flow fields according to *Jay* [2005] and would not have been considered as a single, huge SEE. Two flow fields comprise DG5, and only one comprises DG4.

[59] Conversely, in some cases, flow fields may comprise several directional groups and cannot therefore have been formed in a short interval of time. For instance, DG3 is observed between 705 m (red weathered layer) and 750 m (flow contact with a slightly eroded/weathered top), whereas the flow field was originally identified between 705 m and 785 m (red weathered horizon): DG3 comprises only the lower half of the volcanologically defined flow field [*Jay*, 2005]. Analysis of paleomagnetic directions from the two sites (MB21 and MB15) sampled above DG3 leads us to estimate that a long time interval, at least several centuries,

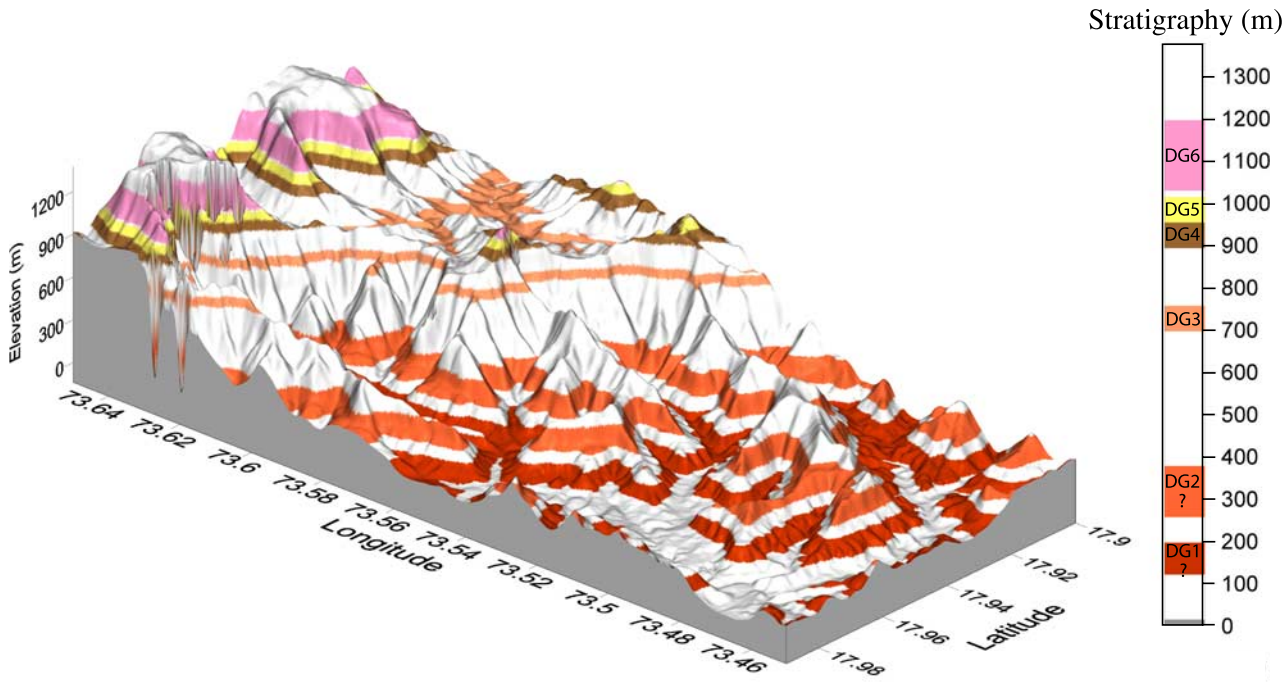

Figure 9. The main volcanic SEEs in the M'war area defined in this work (M'war-Poladpur section) plotted on a 3-D view of topography (Shuttle Radar Topography Mission digital topographic data, NASA).

occurred between emplacement of DG3 and MB21 (angular distance between paleomagnetic directions is 37°) and again between emplacement of MB15 and MB21 (angular distance is about 20°).

[60] In order to determine the volume of DGs, one has to estimate the surface extent of lava units, i.e., their length along the strike of the M'war escarpment and their width perpendicular to it. Paleomagnetic results from the WP section may provide some constraints. On the basis of the respective volcanic architectures of the MP and WP sections, *Jay* [2005] concluded that none of the sheet lobes from the two traverses corresponded, implying that the lateral extent of any individual sheet lobe would be less than the distance between the traverses (~20 km), an observation that is considered typical of basaltic effusive volcanism, as observed elsewhere, for instance in Iceland and Hawaii (T. Thordarson, personal communication, 2006). Although indeed many lava units are not traced from the MP section to the WP section, and despite the limited thickness of the WP section which lies on the eastern side of the main escarpment (with very small slope along the road), our magnetic analysis leads us to propose that actually several thick flow packages can be traced over the 20 km east-west separation between the sections (i.e., perpendicular to the strike of dikes and eruptive fissures along the Mahabaleshwar escarpment). We infer that lavas at these sites are issued from the same flow field and that the corresponding sheet lobes in the two sections were emplaced at the same time (within a timescale on the order of decades) since they recorded the same magnetic direction. The analysis of secular variation is therefore a powerful tool which may allow regional correlations of lava successions and identification of time-equivalent units, which belong to the same stratigraphic unit, over the different traverses.

[61] In addition, regional correlation of time-equivalent units can be used in conjunction with a simplistic geometrical construction (Figure 10) to roughly evaluate the volumes of DGs. The two flow packages for which we propose a correlation between the two sections have larger thicknesses of ~40 and 170 m on one side, and smaller thicknesses on the other side of 20 and >20 m. If we assume that the cross section of a flow field is triangular with maximum thickness in the section where we observe the larger value (Figure 10), the corresponding cross sections range from 2 to 7 km^2. If we further assume that a given flow field extends along the strike of faults and dikes in the ~N-S direction (along the Western Ghats escarpment) for on the order of 200 km (say 100 to 400 km; this is discussed below), we obtain a range of flow field volumes from 400 to 1400 km^3 (or 200 to 2800 km^3 using the range of lengths). Although these values are not well constrained, they happen to be in the range of (though somewhat smaller than) values proposed in a number of recent trap studies: e.g., ~1300 km^3 for the Roza flow in the Columbia Flood Basalt [*Reidel*, 1998; *Thordarson and Self*, 1998; *Self et al.*, 2006], 10^3–10^4 km^3 in several areas of the Deccan Traps [*Jay*, 2005; *Jerram and Widdowson*, 2005; *Self et al.*, 2006] or up to 6300 km^3 as estimated for individual events in the Etendeka and Paranã provinces [*Milner et al.*, 1995].

[62] These estimates are of course quite rough, but many lines of evidence now point in the same direction, i.e., that of extremely voluminous flows in most CFB provinces, and in particular in the Deccan. The question is how much of the total (~800 to 1000 km north-south and ~500 to 1000 km east-west) extent of the traps corresponds to SEEs or large

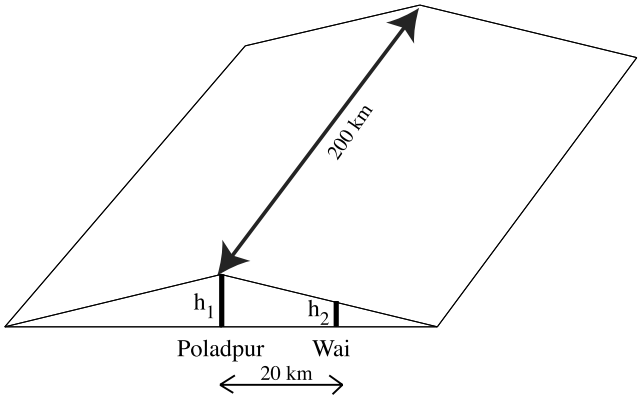

Figure 10. A simple model for a flow field (SEE) with a triangular cross section. Axis is at the Mahabaleshwar escarpment (larger thickness). The thicknesses of the flow field are supposed to be h_1 at P and h_2 at W. The along-strike distance is evaluated as being ~200 km (see text).

flow packages. Outcrops to the east, such as the Rajahmundry traps, bear evidence of magma transport over very large distances [*Baksi*, 2001; *Knight et al.*, 2003; *Baksi*, 2005; *Knight et al.*, 2005; *Jay and Widdowson*, 2007]. This is reinforced by the fact that dike-feeder systems are uncommon east of the main escarpment and that traps thin considerably to the east. This supports the idea that a significant part of the flows were erupted from N-S trending dike systems not far from the present maximum thickness zone, i.e., the escarpment itself. So, the E-W extent of many flows could be on the order of 600 km at the latitude of Mahabaleshwar, and this value can be doubled if a mirror image on the other side of the zone of maximum thickness, corresponding to the part of the traps which has been downfaulted and removed by drift of the Seychelles microcontinent, is invoked. *Mitchell and Widdowson* [1991] and *Jerram and Widdowson* [2005] provide evidence that flow fields may extend over 200 km in the N-S direction. Their reconstruction of the staggered pile of formations (Figure 2a) actually suggests that SEEs may extend up to 400 km in that direction. We have used values of 200 km and 40 km in the N-S and E-W directions respectively in our prior discussion of flow volumes in the MP and WP sections. We have seen that the very poor state of preservation in the WP section unfortunately limited our potential to correlate DGs over a significant horizontal distance, although we did argue that two flow packages could be correlated. With the above values, flow volumes were evaluated as maximum thickness, multiplied by a surface outcrop of $40 \times 200 = 8000$ km^2. The

Table 5. Estimates of Carbon Dioxide and Sulfur Dioxide Degassed During Single Eruptive Events, Single Lava Units (MP Section), and SO_2 Injection by the Chixculub Impact[a]

Event in Poladpur Section	Number of Flows	Thickness, m	Volume, km^3	Eruption Rate (SEE ~ 100 years), km^3/a	Mass CO_2, Gt	Flux CO_2 (N Flows − 1 year Each), Gt/a	Flux CO_2 (N Flows − 10 years Each), Gt/a	Flux CO_2 (SEE ~ 100 years), Gt/a
Pulses								
DG6	7	180	21600	216	297	42.4	4.2	3.0
DG5	3	40	4800	48	66	22.0	2.2	0.7
DG4	3	65	7800	78	107	35.8	3.6	1.1
DG3	3	40	4800	48	66	22.0	2.2	0.7
DG2	5	120	14400	144	198	39.6	4.0	2.0
DG1	3	80	9600	96	132	44.0	4.4	1.3
Individual flow	1	~20	3000	30–300	41	41.3	4.1	
Total flows in the MP section	25		75000		1031	41.3		
Whole MP Ghat section			138000		1898			

Event in Poladpur Section	Number of Flows	Thickness, m	Volume, km^3	Eruption Rate (SEE ~ 100 years), km^3/a	Mass SO_2, Gt	Flux SO_2 (N Flows − 1 year Each), Gt/a	Flux SO_2 (N Flows − 10 years Each), Gt/a	Flux SO_2 (SEE ~ 100 years), Gt/a
Pulses								
DG6	7	180	21600	216	143	20.4	2.0	1.4
DG5	3	40	4800	48	32	10.6	1.1	0.3
DG4	3	65	7800	78	51	17.2	1.7	0.5
DG3	3	40	4800	48	32	10.6	1.1	0.3
DG2	5	120	14400	144	95	19.0	1.9	1.0
DG1	3	80	9600	96	63	21.1	2.1	0.6
Individual flow	1	~20	3000	30–300	20	19.8	2.0	
Total flows in the MP section	25		75000		495			
Whole MP Ghat section			138000		911			
Chicxulub impact					50–540			

[a]Gt, 1 gigaton = 10^{12} kg. Magma density is taken to be 2750 kg m^{-3}. Preeruptive CO_2 concentration is taken to be 0.5 wt % [*Self et al.*, 2006] and SO_2 concentration 1200 ppm [*Bonnefoy*, 2005; *Self et al.*, 2006]. Duration of emplacement of single lava units is based on estimates for the Roza flow field (see text and *Thordarson and Self* [1998]). The range of emplacement durations for single lava units is 1 to 10 years and for SEE 10 to 100 years. The mass of SO_2 due to Chixculub impact is from *Pierazzo et al.* [2003]. The mass of CO_2 in the present-day atmosphere is about 3000 Gt and annual anthropogenic CO_2 emission rate about 30 Gt a^{-1} [*Intergovernmental Panel on Climate Change*, 2001].

above discussion shows that this could possibly be extended to 600 × 400 = 240,000 km^2. In our first estimates, SEE (or DG) volumes ranged from 200 to 2800 km^3. With the revised estimates of lava flow extent, these values can be multiplied by a factor of 60, i.e., 12,000 to 168,000 km^3. One might be reluctant to accept such large estimates until they can be better demonstrated in the field (as will partly be done in our follow up paper on sections further north), and it may be more conservative to stick to the values provided by actual observations of larger flows in the Columbia, Deccan and Parana CFBs (3000 to 20,000 km^3, see above), which happen to range from the upper boundary of estimates with the "small" surface outcrop to the lower boundary of the ones that use the "large" outcrop estimates. Table 5 lists lava volume estimates with a 200 km × 600 km outcrop hypothesis, half of the maximum value invoked above. The uncertainties in these estimates are clearly up to a factor of 2–10 and values should only be used as guidelines in the following. But again, one must realize the mind-boggling size of several flow fields as outlined by the thickest DGs.

[63] Physical volcanology and analysis of paleomagnetic secular variation both place rather stringent upper boundaries on the duration of even the largest flow packages as being on the order of decades to centuries, and in general less than one century, given the recent values of geomagnetic secular variation. This implies lava fluxes on the order of 30 to 200 km^3 a^{-1} if we take a modal duration of 100 years (with the full range of volumes, rates can be up to 1 order of magnitude smaller or two orders of magnitude larger, if one takes the full surface outcrop and a duration reduced to a decade). A magma flux of 100 km^3 a^{-1} is a factor of 5 times greater than the average flux (∼20 km^3 a^{-1}) of the 1783–1784 A.D. Laki eruption, yet compatible with the maximum magma fluxes estimated by *Thordarson and Self* [1993] and compatible with estimates given for the Roza eruption [*Thordarson and Self*, 1996, 1998].

4.3. Climatic Consequences and Concluding Remarks

[64] The impact of volcanism on the environment and in particular on climate is now understood to be mainly linked to the release of gases to the atmosphere. Volcanic gases are dominated by water vapor (H_2O; 50–90%), carbon dioxide (CO_2; 1–40%) and sulfur dioxide (SO_2; 1–25%), with other components in minor concentrations [*Textor et al.*, 2004]. It is now apparent that sulfur probably plays the leading role in climate-volcanism relations [*Rampino and Self*, 1984, 1992; *Rampino and Strothers*, 1988; *Thordarson and Self*, 1993; *Thordarson et al.*, 1996; *Thordarson and Self*, 2003; *Chenet et al.*, 2005; *Self et al.*, 2006]. The actual effects are a function of eruption rate and mechanism. But before analyzing in more detail the potential of SO_2 in flood basalt SEEs, we first briefly review the more abundant CO_2 (Table 5).

[65] Assuming a mass fraction of 0.5% of CO_2 in the melt, *Self et al.* [2006] estimated that about 14 Gt of CO_2 could be released for every km^3 of basaltic lava from the Deccan Traps. Using the same mass fraction, the mass of CO_2 released by a SEE as identified by a paleomagnetic DG ranges from 70 to 300 Gt over a period estimated not to exceed 100 years. The corresponding mean annual flux rates are 1 to 3 Gt a^{-1} for a 100yr duration of each SEE, up to 20 to 45 Gt a^{-1} if each flow unit lasted only 1 year (Table 5). In comparison, the CO_2 flux at mid-ocean ridges is estimated at about 0.097 Gt a^{-1} [*Marty and Tolstikhin*, 1998]. The successive DGs and individual lava flows as a whole would have released almost 2000 Gt over a period that could have lasted from as little as a few thousand years to more than 100 ka (duration of big RB formation). This release of carbon dioxide is currently invoked to explain the warming period during the late Maastrichtian (see *Wignall* [2001] for a synthesis). But overall, CO_2 is not any more considered as the leading agent of climate and environmental change, particularly its consequences on the biosphere, at the time of mass extinction.

[66] Our current understanding of the deleterious consequences of SO_2 emission is based on recent and historical volcanic eruptions [*Robock*, 2000]. One of the highest SO_2 emission rates occurred during the 1783 Laki volcanic eruption [*Thordarson et al.*, 1996], which caused drastic climate changes over the northern hemisphere, for instance an exceptionally hot summer followed by a very cold winter over Europe, and anomalous numbers of human deaths, due to acid haze and ensuing respiratory diseases in western Europe or starvation in Japan and Alaska [e.g., *Thordarson and Self*, 1993; *Grattan and Charman*, 1994; *Thordarson and Self*, 2003; *Chenet et al.*, 2005; *Grattan et al.*, 2005; *Oman et al.*, 2006a, 2006b].

[67] The amount of SO_2 released by flows in continental flood basalt provinces has long remained ill-constrained because flood basalts are often badly preserved and contain almost no fluid inclusions that could be used to estimate both the preeruptive and released amounts of volatiles. The first estimate of the amount of sulfur released in the atmosphere by a CFB was obtained by *Thordarson and Self* [1996] on the well-preserved porphyritic Roza flow field in the Columbia River. These authors were able to propose that the 1300 km^3 flow released 12 Gt of SO_2 over a decade or even less. The annual emission rate would have reached 1.2 Gt a^{-1} at least. More recently, *Bonnefoy* [2005], *Self et al.* [2006], and E. Humler (personal communication, 2005) have proposed several chemical proxies, based on composition of fluid inclusions or glass in recent basaltic flows or FeO content in older ones, to estimate the original sulfur concentration of CFBs. All find values on the order of 1000 ppm (typical of ocean island basalts) for the Deccan lavas. This allows one to convert lava volumes and fluxes to sulfur (or SO_2, or H_2SO_4 aerosol as the conversion proceeds) volumes and fluxes injected into the atmosphere (Table 5). The resulting range of SO_2 emissions for individual DGs is from 30 to 140 Gt, implying fluxes from 0.3 to 1.4 Gt a^{-1} (mean ∼1 Gt a^{-1}) if duration of SEE was 100 years, 3 to 14 Gt a^{-1} (mean ∼ 8 Gt a^{-1}) if duration of SEE was only 10 years. Each one of the 25 single lava units of the MP section not belonging to DGs could have released ∼20 Gt of SO_2 in 1 to 10 years (flux of ∼2 to ∼20 Gt a^{-1}). The amount of SO_2 released to the atmosphere by individual Deccan trap DGs is larger than that emitted by the Roza flow field because of larger size and longer duration (assuming a century in the case of DGs, a decade in the case of the Roza flow field). But the annual mean emission rate (1 to 20 Gt a^{-1} in the case of DGs and possibly also single flow units) is similar to that of the Roza flow field and vindicates the estimates of *Self et al.* [2006] (0.5 to 3 Gt a^{-1}). As a whole, the total SO_2 output from the lava pile sampled

along the MP section may have been on the order of 900 Gt, emitted over some 1000 years (or less) of (temporally highly non uniform) volcanic activity.

[68] In comparison, *Ivanov et al.* [1996], *Yang and Ahrens* [1998], and *Pierazzo et al.* [2003] estimated that the meteorite which impacted sulfate-rich sediments (anhydrites) and formed the Chicxulub crater might have vaporized 50 to 540 Gt of SO_2. In these models, sulfur release would have been quasi-instantaneous (a timescale well under a year), but it should extend to decades and up to a century for individual Deccan SEEs. Moreover, for very large amounts of SO_2, the conversion time of SO_2 to H_2SO_4 aerosol becomes much longer: as a result, the duration of climatic effects in case of impact can extend to decades. Orders of magnitude for SO_2 release from the Deccan eruptions and Chicxulub may not be as different as has often been supposed so far: the lower values of Chicxulub SO_2 release estimates are only 3 times smaller than the upper estimates for the largest flow package (DG6); and the respective timescales could be as close as 1 and 10 years. Importantly, they may be even more similar, when conversion time is taken into account, because many authors have previously thought that the values were more like one second versus a million years. Moreover, there was only one impact, whereas there was a succession of SEEs and flows in the Deccan Traps. The 1200-m-thick MP section represents only one third of the total trap sequence and volume. And the lower Formations of the Deccan appear to be characterized by even more massive SEEs with even fewer quiescence periods (as will be documented in a future paper on sections farther north).

[69] The fluxes implied by the thickest SEEs (2 to 20 Gt a^{-1} of SO_2 for 10 to 100 years) can be compared with the fluxes due to the 1783 Laki eruption (0.1 Gt over 8 months), or to the anthropogenic annual emission rate of SO_2 (0.1 Gt in 1985 [*Benkovitz et al.*, 1996]). The very high emission rates typical of the Deccan SEEs have (fortunately) not been observed during the past millennia. The only known event which emitted large amounts of SO_2 is the Toba eruption, some 71,500 years ago, which released about 1 Gt of SO_2 to the atmosphere over a period as short as a year [*Rampino and Self*, 1992]. Climate modeling may help to better quantify the impact of such supereruptions. *Jones et al.* [2005] have shown that the Toba eruption deeply affected the Earth's radiative budget, leading to global cooling by about 17°C or more 1 year after the onset of eruption and up to 2°C after 10 years. Drastic precipitation changes are also found in these climate simulations. A SEE in the Deccan Traps could have released an annual amount of SO_2 at least similar to that of Toba and possibly larger by more than an order of magnitude, lasting over a decade or more.

[70] A significant remaining question regarding the eruptive sequence would be to compare the time spacing between SEEs and flows with the typical time (estimated to be on the order of 1000 years) over which the global ocean can reach equilibrium after a major perturbation. A SEE, however large, may not be able by itself to trigger a mass extinction. The very large Roza flow field, or for that matter the entire Columbia flood basalt (the smallest of all flood basalts by an order of magnitude), however severe their environmental impact, did not trigger a mass extinction. Actually some full-sized traps do not trigger a major event [e.g., *Courtillot and Renne*, 2003]. Discrete volcanic SEEs would have been additive only (and would not lead to a runaway mode) if they were separated by enough time for the system, including the oceans, to return to equilibrium prior to the next eruptive event.

[71] If sulfur yield is indeed an indication of the severity of environmental change, the fact that the Chicxulub impactor may not have yielded considerably more gases than a large SEE would imply that it could not by itself have generated a mass extinction. We suggest that it is because impact fell in the middle of the ongoing Deccan trap eruptions [*Courtillot et al.*, 1988; *Bhandari et al.*, 1995, 1996; *Courtillot et al.*, 2000], i.e., in a highly stressed world where pollution was already massive and extinctions had started, that it did trigger its own large wave of extinction. And as far as flood basalts are concerned, it may be necessary for several SEEs to occur within less than the time needed for the ocean to reequilibrate for a runaway effect to occur, leading to an actual mass extinction. The detailed signature of the sequence of SEEs may therefore be the key to explain the difference in environmental impact of otherwise rather similar flood basalts. The present study has been a first attempt at better constraining this time signature, even though it appears a priori beyond the reach and resolving power of the best current geochronological techniques.

[72] Finally, we wish to emphasize the potential relevance of such work to ongoing studies of climate change. It has long been thought that study of trap volcanism could not have much relevance to current climate studies, because of vastly different timescales. The enormous volumes and short durations of emplacement of trap flows imply injection rates well in excess of current rates and timescales of decades which are quite relevant to climatic studies. It may therefore be that further detailed analysis of the geological and biotic signatures of such events would provide climate modelers with important benchmarks.

[73] **Acknowledgments.** We sincerely thank Sunil Bajpai and Syed Khadri for their considerable help in fieldwork and for extensive discussions. Anne Jay provided very substantial assistance with chemostratigraphy and joined in our first field trip. We are grateful to Hélène Bouquerel for technical and field assistance and to Jean Besse for discussions on paleomagnetic data and analyses and for joining us during the first field trip. Steve Self contributed very helpful comments, encouragement, and suggestions throughout much of this study. We acknowledge unusually careful and detailed reviews by Mike Widdowson and Thor Thordarson and advice from Associate Editor Bob Duncan, which led to clarification of the first draft of the paper. Funding was obtained by a CNRS-ECLIPSE program. This is IPGP contribution 2220.

References

Alvarez, L. W., W. Alvarez, F. Asarao, and H. V. Michel (1980), Extraterrestrial causes of the Cretaceous/Tertiary extinction, *Science*, *208*, 1095–1108.

Baksi, A. K. (2001), The Rajahmundry Traps, Andhra Pradesh: Evaluation of their petrogenesis relative to the Deccan Traps, *Proc. Indian Acad. Sci.*, *110*(4), 397–407.

Baksi, A. K. (2005), Comment on "$^{40}Ar/^{39}Ar$ dating of the Rajamundry Traps, eastern India and their relationship to the Deccan Traps" by Knight et al. (EPSL, 2008 (2003) 85–99), *Earth Planet. Sci. Lett.*, *239*, 368–373.

Beane, J. E., C. A. Turner, P. R. Hooper, K. V. Subbarao, and J. N. Walsh (1986), Stratigraphy, composition and form of the Deccan basalts, Western Ghats, Deccan, India, *Bull. Volcanol.*, *48*, 61–83.

Becker, L., R. J. Poreda, A. R. Basu, K. O. Pope, T. M. Harrison, C. Nicholson, and R. Iasky (2004), Bedout: A possible end-Permian impact crater offshore of northwestern Australia, *Science*, *304*, 1469–1475.

Bekki, S., R. Toumi, and J. A. Pyle (1993), Role of sulphur photochemistry in tropical ozone changes after the eruption of Mount Pinatubo, *Nature*, *362*, 331–333.

Benedetti, M. F., et al. (2003), Chemical weathering of basaltic lava flows undergoing extreme climatic conditions: The water geochemistry record, *Chem. Geol.*, *201*, 1–17.

Benkovitz, C. M., M. T. Scholtz, J. Pacyna, L. Tarrason, J. Dignon, E. C. Voldner, P. A. Spiro, J. A. Logan, and T. E. Graedel (1996), Global gridded inventories of anthropogenic emissions of sulphur and nitrogen, *J. Geophys. Res.*, *101*, 29,239–29,253.

Besse, J., and V. Courtillot (2002), Apparent and true polar wander and the geometry of the geomagnetic field over the last 200 Myr, *J. Geophys. Res.*, *107*(B11), 2300, doi:10.1029/2000JB000050.

Bhandari, N., P. N. Shukla, Z. G. Ghevariya, and S. M. Sundaram (1995), Impact did not trigger Deccan volcanism: Evidence from Anjar K/T boundary intertrappean sediments, *Geophys. Res. Lett.*, *22*(4), 433–436.

Bhandari, N., P. N. Shukla, Z. G. Ghevariya, and S. M. Sundaram (1996), K/T boundary layer in Deccan intertrappeans at Anjar, Kutch, *Spec. Pap. Geol. Soc. Am.*, *307*, 417–424.

Bodas, M. S., S. F. R. Khadri, and K. V. Subbarao (1988), Stratigraphy of the Jawhar and Igatpuri formations, Western Ghats lava pile, India, in *Deccan Flood Basalts*, edited by K. V. Subbaro, *Mem. Geol. Soc. India*, *10*, 235–252.

Bonnefoy, B. (2005), Evolution geochimique des laves des trapps du Deccan et determination des concentrations en S, F et Cl dans des inclusions vitreuses de Rajahmundry, Master thesis, Inst. de Phys. du Globe de Paris, Paris.

Cande, S., and D. V. Kent (1995), Revised calibration of the geomagnetic polarity timescale for the Late Cretaceous and Cenozoic, *J. Geophys. Res.*, *100*, 6093–6095.

Chenet, A. L. (2006), Reconstruction de la séquence éruptive des Traps du Deccan, Inde: Conséquences climatiques et environnementales, Ph.D. thesis, 390 pp., Inst. de Phys. du Globe de Paris, Paris.

Chenet, A. L., V. Courtillot, and F. Fluteau (2005), Modelling massive sulphate aerosol pollution, following the large 1783 Laki basaltic eruption, *Earth Planet. Sci. Lett.*, *236*, 721–731, doi:10.1016/j.epsl.2005.04.046.

Chenet, A. L., X. Quidelleur, F. Fluteau, V. Courtillot, and S. Bajpai (2007), ^{40}K-^{40}Ar dating of the main Deccan large igneous province: Further evidence of KTB age and short duration, *Earth Planet. Sci. Lett.*, *263*, 1–15, doi:10.1016/j.epsl.2007.07.011.

Cogné, J. P. (2003), PaleoMac: A Macintosh™ application for treating paleomagnetic data and making plate reconstructions, *Geochem. Geophys. Geosyst.*, *4*(1), 1007, doi:10.1029/2001GC000227.

Courtillot, V. (1994), Mass extinctions in the last 300 million years: One impact and seven flood basalt?, *Irs. J. Earth Sci.*, *43*, 255–266.

Courtillot, V. (1999), *Evolutionary Catastrophes: The Science of Mass Extinctions*, 173 pp., Cambridge Univ. Press, New York.

Courtillot, V., and P. Renne (2003), On the ages of flood basalt events, *C. R. Acad. Sci.*, *335*(1), 113–140.

Courtillot, V., and T. Thordarson (2005), Flood basalts appear to be the main cause of biological mass extinctions in the Phanerozoic, paper presented at European Geosciences Union 2005, Vienna, Austria, 24–29 April.

Courtillot, V., J. Besse, D. Vandamme, R. Montigny, J.-J. Jaeger, and H. Cappetta (1986), Deccan flood basalts at the Cretaceous/Tertiary boundary?, *Earth Planet. Sci. Lett.*, *80*, 361–374.

Courtillot, V., G. Feraud, H. Maluski, D. Vandamme, M. G. Moreau, and J. Besse (1988), Deccan flood basalts and the Cretaceous/Tertiary boundary, *Nature*, *333*, 843–846.

Courtillot, V., Y. Gallet, R. Rocchia, G. Feraud, E. Robin, C. Hoffman, N. Bhandari, and Z. G. Ghevariya (2000), Cosmic markers, ^{40}Ar/^{39}Ar dating and paleomagnetism of the KT sections in the Anjar Area of the Deccan large igneous province, *Earth Planet. Sci. Lett.*, *182*, 137–156.

Cox, K. G., and C. J. Hawkesworth (1984), Relative contribution of crust and mantle to flood basalt magmatism, Mahabaleshwar area, Deccan Traps, *Philos. Trans. R. Soc. London, Ser. A*, *310*, 627–641.

Cox, K. G., and C. J. Hawkesworth (1985), Geochemical stratigraphy of the Deccan Traps at Mahabaleshwar, Western Ghats, India, with implications for open system magmatic processes, *J. Petrol.*, *26*, 355–377.

Cripps, J. A., M. Widdowson, R. A. Spicer, and D. W. Jolley (2005), Coastal ecosystem responses to late stage Deccan Trap volcanism: The post K–T boundary (Danian) palynofacies of Mumbai (Bombay), west India, *Palaeogeogr. Palaeoclimatol. Palaeoecol.*, *216*, 303–332.

Day, R., M. D. Fuller, and V. A. Schmidt (1977), Hysteresis properties of titanomagnetites: Grain size and composition dependence, *Phys. Earth Planet. Inter.*, *13*, 260–267.

Dessert, C., B. Dupré, L. M. François, J. Schott, G. Gaillardet, J. Chakrapani, and S. Badjope (2001), Erosion of Deccan Trapps determined by river geochemistry: Impact on the global climate and oceanic ^{87}Sr/^{86}Sr, *Earth Planet. Sci. Lett.*, *188*, 83–98.

Devey, C. W., and P. C. Lightfoot (1986), Volcanology and tectonic control of stratigraphy and structure in the western Deccan Traps, *Bull. Volcanol.*, *48*, 195–207.

Donnadieu, Y., R. Pierrehumbert, R. Jacob, and F. Fluteau (2006), Modelling the primary control of paleogeography on Cretaceous climate, *Earth Planet. Sci. Lett.*, *248*, 426–437, doi:10.1016/j.epsl.2006.06.007.

Duncan, R. A., and D. G. Pyle (1988), Rapid eruption of the Deccan flood basalts at the Creatceous/Tertiary boundary, *Nature*, *333*, 841–843.

Dunlop, D. J., and Ö. Özdemir (1997), *Rock Magnetism: Fundamentals and Frontiers*, 573 pp., Cambridge Univ. Press, New York.

Erwin, D. H. (2004), Mass extinctions and evolutionary radiations, in *Evolution From Molecules to Ecosystems*, edited by A. Moya and E. Font, pp. 218–228, Oxford Univ. Press, New York.

Farley, K. A., P. Ward, G. Garrison, and S. Mukhopadhyay (2005), Absence of extraterrestrial ^{3}He in Permian-Triassic age sedimentary rocks, *Earth Planet. Sci. Lett.*, *240*, 265–275.

Féraud, G., and V. Courtillot (1994), Comment on: "did Deccan volcanism pre-date the Cretaceous-Tertiary transition?," *Earth Planet Sci. Lett.*, *122*, 259–262.

Fisher, R. A. (1953), Dispersion on a sphere, *Proc. R. Soc. London, Ser. A*, *217*, 295–305.

Fluteau, F. (2006), Climatic consequences on trap emplacement: The case of Deccan, paper presented at International Conference on Continental Volcanism, Int. Assoc. of Volcanol. and Chem. of the Earth's Inter., Guangzhou, China, 14–18 May.

Gallet, Y., A. Genevey, and M. L. Goff (2002), Three millennia of directional variation of the Earth's magnetic field in western Europe as revealed by archeological artefacts, *Phys. Earth Planet. Inter.*, *131*, 81–89.

Genevey, A., and Y. Gallet (2002), Intensity of the geomagnetic field in western Europe over the past 2000 years: New data from ancient French pottery, *J. Geophys. Res.*, *107*(B11), 2285, doi:10.1029/2001JB000701.

Gérard, M., et al. (1999), The weathering of Mount Cameroon-1–Mineralogy and geochemistry, in *Geochemistry of the Earth's Surface*, edited by H. Ármannsson, pp. 381–384, A. A. Balkema, Rotterdam.

Gérard, M., S. Caquineau, A. L. Chenet, F. Fluteau, V. Courtillot, and K. V. Subbarao (2006), Red boles in the Deccan Traps: Time constraints from alteration processes, paper presented at European Geosciences Union 2006, Vienna, Austria, 2–7 April.

Gérard, M., S. Caquineau, J. Pinheiro, and G. Stoops (2007), Weathering and allophane neoformation in soils on volcanic ash from the Azores, *Eur. J. Soil Sci.*, *58*, 496–515.

Gosh, P., M. R. G. Sayyed, R. Islam, and S. M. Hundekari (2006), Inter-basaltic caly (bole bed) horizons from Deccan Traps of India: Implications for paleo-weathering and paleo-climate during Deccan volcanism, *Palaeogeogr. Palaeoclimatol. Palaeoecol.*, *242*, 90–109.

Grattan, J., and D. J. Charman (1994), Non-climatic factors and the environmental impact of volcanic volatiles: Implications of the Laki fissure eruption of AD 1783, *Holocene*, *4*, 101–106.

Grattan, J., R. Rabartin, S. Self, and T. Thordarson (2005), Volcanic air pollution and mortality in France 1783–84, *C. R. Geosci.*, *337*, 641–651.

Halls, C. (1978), The use of converging remagnetization circles in palaeomagnetism, *Phys. Earth Planet. Inter.*, *16*, 1–11.

Hofmann, C., V. Courtillot, G. Feraud, P. Rochette, G. Yirgu, E. Ketefo, and R. Pik (1997), Timing of the Ethiopian flood basalt event and implications for plume birth and global change, *Nature*, *389*, 838–841.

Hofmann, C., G. Féraud, and V. Courtillot (2000), ^{40}Ar/^{39}Ar dating of mineral separates and whole rocks from the Western Ghats lava pile: Further constraints on duration and age of the Deccan Traps, *Earth Planet. Sci. Lett.*, *180*, 13–27.

Inamdar, P. M., and D. Kumar (1994), On the origin of bole in Deccan Traps, *J. Geol. Soc. India*, *44*, 331–334.

Intergovernmental Panel on Climate Change (2001), *Climate Change, radiative forcing of climate change: The Scientific Assessment*, Cambridge Univ. Press, New York.

Ivanov, B. A., D. D. Badukov, O. I. Yakovlev, M. V. Gerasimov, Y. P. Pope, and A. C. Ocampo (1996), Degassing of sedimentary rocks due to Chicxulub impact: Hydrocode and physical simulations, *Spec. Pap. Geol. Soc. Am.*, *307*, 125–138.

Jay, A. E. (2005), Volcanic architecture of the Deccan Traps, Western Maharashtra, India: An integrated chemostratigraphic and palaeomagnetic study, Ph.D. thesis, 346 pp., Open Univ., Milton Keynes, UK.

Jay, A. E., and M. Widdowson (2007), Stratigraphy, structure, and volcanology of the south-east Deccan continental flood basalt province: Implications for eruptive extent and volumes, *J. Volcanol. Geotherm. Res.*, *165*, 177–188.

Jerram, D. A., and M. Widdowson (2005), The anatomy of Continental Flood Basalt Provinces: Geological constraints on the processes and products of flood volcanism, *Lithos*, *79*, 385–405.

Jones, G. S., J. M. Gregory, P. A. Stott, S. F. B. Tett, and R. B. Thorpe (2005), An AOGCM simulation of the climate response to a volcanic super-eruption, *Clim. Dyn.*, *25*, 725–738.

Kamo, S. L., G. K. Czamanske, Y. Amelin, V. A. Fedorenko, D. W. Davis, and V. R. Trofimov (2003), Rapid eruption of Siberian flood-volcanic rocks and evidence for coincidence with the Permian-Triassic boundary and mass extinction at 251 Ma, *Earth Planet. Sci. Lett.*, *214*(1–2), 75–91.

Keller, G., W. Stinnesbeck, T. Adatte, and D. Stüben (2003), Multiple impacts across the Cretaceous-Tertiary boundary, *Earth Sci. Rev.*, *62*, 327–363.

Khadkikar, A. S., D. A. Sant, V. Gogte, and R. V. Karanth (1999), The influence of Deccan volcanism on climate: Insights from lacustrine intertrappean deposits, Anjar, western India, *Palaeogeogr. Palaeoclimatol. Palaeoecol.*, *147*, 141–149.

Khadri, S. F. R., K. V. Subbarao, and M. S. Bodas (1988), Magnetic studies on a thick pile of Deccan trap flows at Kalsubai, in *Deccan Flood Basalts*, edited by K. V. Subbaro, *Mem. Geol. Soc. India*, *10*, 163–189.

Khadri, S. F. R., J. N. Walsh, and K. V. Subbarao (1999), Chemical and magneto-stratigraphy of Malwa Traps around Mograba region, Dhar District (M. P.), *Mem. Geol. Soc. India*, *43*, 203–218.

Kirchner, I., G. L. Stenchikov, H.-F. Graf, A. Robock, and J. C. Antuna (1999), Climate model simulation of winter warming and summer cooling following the 1991 Mount Pinatubo volcanic eruption, *J. Geophys. Res.*, *104*, 19,039–19,055.

Kirschvink, J. L. (1980), The least squares line and plane and the analysis of palaeomagnetic data, *Geophys. J. R. Astron. Soc.*, *62*, 699–718.

Knight, K. B., P. R. Renne, A. Halkett, and N. White (2003), $^{40}Ar/^{39}Ar$ dating of the Rajamundry Traps, eastern India and their relationship to the Deccan Traps, *Earth Planet. Sci. Lett.*, *208*, 85–99, doi:10.1016/S0012-821X(02)01154-8.

Knight, K. B., S. Nomade, P. R. Renne, A. Marzoli, H. Bertrand, and N. Youbi (2004), The central Atlantic magmatic province at the Triassic–Jurassic boundary: Paleomagnetic and $^{40}Ar/^{39}Ar$ evidence from Morocco for brief, episodic volcanism, *Earth Planet. Sci. Lett.*, *228*, 143–160, doi:10.1016/j.epsl.2004.09.022.

Knight, K. B., P. Renne, J. Baker, T. Waight, and N. White (2005), Reply to '$^{40}Ar/^{39}Ar$ dating of the Rajahmundry Traps, eastern India and their relationship to the Deccan Traps: Discussion' by A. K. Baksi, *Earth Planet. Sci. Lett.*, *239*, 374–382, doi:10.1016/j.epsl.2005.08.013.

Kono, M., H. Kinoshita, and Y. Aoki (1972), Paleomagnetism of the Deccan Trap basalts in India, *J. Geomagn. Geoelectr.*, *24*, 49–67.

Macleod, N. (2004), A statistical evaluation of the association between LIP volcanism and extinction-intensity peaks over the last 250 My, paper presented at 32nd International Geological Congress, Florence, Italy, 20–28 Aug.

Mahoney, J. J., J. D. MacDougall, G. W. Lugmair, A. V. Murali, M. Sankardas, and K. Gopalan (1982), Origin of the Deccan Trap flows at Mahabaleshwar inferred form Nd and Sr isotopic and chemical evidence, *Earth Planet. Sci. Lett.*, *60*, 47–60.

Mankinen, E. A., M. Prévot, C. S. Grommé, and R. Coe (1985), The Steen's Mountain (Oregon) geomagnetic polarity transition: 1. Directional history, duration of episodes, and rock magnetism, *J. Geophys. Res.*, *90*, 10,393–10,416.

Marty, B., and I. N. Tolstikhin (1998), CO_2 fluxes from mid-ocean ridges, arcs and plumes, *Chem. Geol.*, *145*, 233–248.

McElhinny, M. W. (1968), Northward drift of India—Examination of recent palaeomagnetic results, *Nature*, *217*, 342–344.

McFadden, P. L., and M. W. McElhinny (1990), Classification of the reversal test in palaeomagnetism, *Geophys. J. Int.*, *103*, 725–729.

McFadden, P. L., R. T. Merill, M. W. McElhinny, and L. Sunhee (1991), Reversal of the Earth's magnetic field and temporal variations of the dynamo families, *J. Geophys. Res.*, *96*, 3923–3933.

McLean, D. M. (1985), Deccan Traps mantle degassing in the terminal Cretaceous marine extinctions, *Cretaceous Res.*, *6*, 235–259.

Mélières, F., and A. Person (1978), Genèse de smectites ferrifères par altération deutérique de la base de coulées volcaniques du Massif Central français, *Rev. Geogr. Phys. Geol. Dyn.*, *20*(5), 389–398.

Merrill, R. T., M. W. McElhinny, and P. L. McFadden (1996), *The Magnetic Field of the Earth*, 531 pp., Academic, San Diego, Calif.

Milner, S. C., A. R. Duncan, A. M. Whittingham, and A. Ewart (1995), Trans-Atlantic correlation of eruptive sequences and individual silicic volcanic units within the Parana-Etendeka igneous province, *J. Volcanol. Geotherm. Res.*, *69*, 137–157.

Mitchell, C., and M. Widdowson (1991), A geological map of the southern Deccan Traps, India and its structural implications, *J. Geol. Soc. London*, *148*, 495–505.

Mohapatra, B. K., and K. K. K. Nair (1996), Some observations on bole beds in Deccan Traps, *Gondwana Geol. Mag. Spec. Publ.*, *2*, 531–534.

Najafi, S. J., K. G. Cox, and R.N. Sukheswala (1981), Geology and geochemistry of the basalt flows (Deccan Traps) of the Mahad-Mahabaleshwar section, India, in *Deccan Volcanism and Related Provinces in Other Parts of the World*, edited by K. V. Subbarao and R. N. Sukheswala, *Mem. Geol. Soc. India*, *3*, 300–315.

Nomade, S., K. B. Knight, E. Beutel, P. R. Renne, C. Verati, G. Féraud, A. Marzoli, N. Youbi, and H. Bertrand (2007), Chronology of the central Atlantic magmatic province: Implications for the central Atlantic rifting processes and the Triassic–Jurassic biotic crisis, *Palaeogeogr. Palaeoclimatol. Palaeoecol.*, *244*, 326–344.

Oman, L., A. Robock, G. L. Stenchikov, and T. Thordarson (2006a), High-latitude eruptions cast shadow over the African monsoon and the flow of the Nile, *Geophys. Res. Lett.*, *33*, L18711, doi:10.1029/2006GL027665.

Oman, L., A. Robock, G. L. Stenchikov, T. Thordarson, D. Koch, D. T. Shindell, and C. Gao (2006b), Modeling the distribution of the volcanic aerosol cloud from the 1783–1784 Laki eruption, *J. Geophys. Res.*, *111*, D12209, doi:10.1029/2005JD006899.

Pal, P. C. (1969), Palaeomagnetic of the Deccan flood basalts, *Nature*, *223*, 820–822.

Pande, K. (2002), Age and duration of the Deccan Traps, India: A review of radiometric and paleomagnetic constraints, *Proc. Indian Acad. Sci.*, *111*, 115–123.

Perkins, M. E., W. P. Nash, F. H. Brown, and R. J. Fleck (1995), Fallout tuffs of Trapper Creek, Idaho: Record of Miocene explosive volcanism in the Snake River Plain volcanic province, *Geol. Soc. Am. Bull.*, *110*, 344–360.

Pierazzo, E., A. N. Hahamann, and L. C. Sloan (2003), Chicxulub and climate: Radiative perturbations of impact-produced S-bearing gases, *Astrobiology*, *3*(1), 99–117.

Rampino, M. R., and S. Self (1984), Sulphur-rich volcanic eruptions and stratospheric aerosols, *Nature*, *310*, 677–679, doi:10.1038/310677a0.

Rampino, M. R., and S. Self (1992), Volcanic winter and accelerated glaciation following the Toba super-eruption, *Nature*, *359*, 50–52.

Rampino, M. R., and S. Self (2000), Volcanism and biotic extinctions, in *The Encyclopedia of Volcanoes*, edited by H. Sigurdson et al., pp. 263–269, Academic, London.

Rampino, M. R., and R. B. Stothers (1988), Flood basalt volcanism during the past 250 million years, *Science*, *241*, 663–668.

Reidel, S. P. (1998), Emplacement of Columbia River flood basalt, *J. Geophys. Res.*, *103*, 27,393–27,410.

Renne, P., C. C. Swisher, A. L. Deino, D. B. Karner, T. L. Owens, and D. J. DePaolo (1998), Intercalibration of standards, absolute ages and uncertainties in $^{40}Ar/^{39}Ar$ dating, *Chem. Geol.*, *145*, 117–152.

Retallack, G. J. (1991), Untangling the effects of burial alteration and ancient soil formation, *Annu. Rev. Earth Planet. Sci.*, *19*, 183–206.

Riisager, P., A. Riisager, N. Abrahamsen, and R. Waagstein (2002), New paleomagnetic pole and magnetostratigraphy of Faroe Islands flood volcanics, North Atlantic igneous province, *Earth Planet. Sci. Lett.*, *201*(2), 261–276.

Riisager, J., P. Riisager, and A. K. Pedersen (2003a), Paleomagnetism of large igneous provinces: Case-study from West Greenland, North Atlantic igneous province, *Earth Planet. Sci. Lett.*, *214*(3–4), 409–425, doi:10.1016/S0012-821X(03)00367-4.

Riisager, P., S. Hall, M. Antretter, and X. Zhao (2003b), Paleomagnetic paleolatitude of Early Cretaceous Ontong Java Plateau basalts: Implications for Pacific apparent and true polar wander, *Earth Planet. Sci. Lett.*, *208*(3–4), 235–252, doi:10.1016/S0012-821X(03)00046-3.

Riisager, P., K. B. Knight, J. A. Baker, I. U. Peate, M. Al-Kadasi, A. Al-Subbary, and P. R. Renne (2005), Paleomagnetism and $^{40}Ar/^{39}Ar$ Geochronology of Yemeni Oligocene volcanics: Implications for timing and duration of Afro-Arabian traps and geometry of the Oligocene paleomagnetic field, *Earth Planet. Sci. Lett.*, *237*(3–4), 647–672, doi:10.1016/j.epsl.2005.06.016.

Robock, A. (2000), Volcanic eruptions and climate, *Rev. Geophys.*, *38*(2), 191–219.

Rodriguez, E., C. S. Morris, J. E. Belz, E. C. Chapin, J. M. Martin, W. Daffer, and S. Hensley (2005), An assessment of the SRTM topographic products, *JPL Tech. Rep. D-31639*, 143 pp., Jet Propul. Lab., Pasadena, Calif.

Ross, P. S., I. Ukstins Peate, M. K. MacClintock, Y. G. Xu, I. P. Skilling, J. D. L. White, and B. F. Houghton (2005), Mafic volcaniclastic deposits in flood basalt provinces: A review, *J. Volcanol. Geotherm. Res.*, *145*(3–4), 281–314.

Salil, M. S., J. P. Shrivastava, and S. K. Pattanayak (1997), Similarities in the mineralogical and geochemical attributes of detrital calys of Maastrichtian Lameta Beds and weathered Deccan basalt, central India, *Chem. Geol.*, *136*, 25–32.

Sayyed, M. R. G., and S. M. Hundekari (2006), Preliminary comparison of ancient bole beds and modern soils developed upon the Deccan volcanic basalts around Pune (India): Potential for palaeoenvironmental reconstruction, *Quat. Int.*, *156–157*, 189–199, doi:10.1016/j.quaint.2006.05.030.

Schöps, D., Herzig, P. Halbach, G. Friedrich, and N. Blum (1993), Mineralogy, chemistry and oxygen isotope thermometry of nontronite smectites from Central Pacific seamounts, *Chem. Geol.*, *106*, 331–343.

Self, S., T. Thordarson, and L. P. Keszthelyi (1997), Emplacement of continental flood basalt lava flows, in *Large Igneous Provinces; Continental, Oceanic, and Planetary Flood Volcanism*, *Geophys. Monogr. Ser.*, vol. 100, edited by J. Mahoney and M. F. Coffin, pp. 381–410, AGU, Washington, D. C.

Self, S., T. Thordarson, M. Widdowson, and A. Jay (2006), Volatile fluxes during flood basalt eruptions and potential effects on the global environment: A Deccan perspective, *Earth Planet. Sci. Lett.*, *248*, 518–532, doi:10.1016/j.epsl.2006.05.041.

Self, S., A. Jay, M. Widdowson, and L. Keszthelyi (2008), The longest and largest lava flows on Earth, *J. Volcanol. Geotherm. Res.*, in press.

Sethna, S. F. (1999), Geology of Mumbai and surrounding areas and its position in the Deccan Traps stratigraphy, *J. Geol. Soc. India*, *53*, 359–365.

Sheldon, N. D. (2003), Pedogenesis and geochemical alteration of the Picture Gorge subgroup, Columbia River basalt, Oregon, *Geol. Soc. Am. Bull.*, *115*, 1377–1387.

Sheldon, N. D. (2005), Do red beds indicate paleoclimatic conditions? A Permian case study, *Palaeogeogr. Palaeoclimatol. Palaeoecol.*, *228*, 305–319.

Shepard, F. P. (1963), *Submarine Geology*, 557 pp., Harper and Row, New York.

Singh, S. D. (2000), Petrography and clay mineralogy of intertrappean beds of Mumbai, India, *J. Geol. Soc. India*, *55*, 275–288.

Smit, J. (1999), The global stratigraphy of the Cretaceous-Tertiary boundary impact ejecta, *Annu. Rev. Earth Planet. Sci.*, *27*, 75–113.

Stothers, R. B., J. A. Wolff, S. Self, and M. R. Rampino (1986), Basaltic fissure eruptions, plume heights, and atmospheric aerosols, *Geophys. Res. Lett.*, *13*, 725–728.

Subbarao, K. V., and P. R. Hooper (1988), Reconnaissance map of the Deccan Basalt Group in the Western Ghats, India, in *Deccan Flood Basalts*, edited by K. V. Subbaro, *Mem. Geol. Soc. India*, *10*, enclosure.

Subbarao, K. V., D. Chandrasekharam, P. Navaneethakrishnan, and P. R. Hooper (1994), *Stratigraphy and Structure of Parts of the Central Deccan Basalt Province: Eruptive Models*, 321–332 pp., Wiley Eastern, New Delhi.

Subbarao, K. V., M. S. Bodas, S. F. R. Khadri, and J. E. Beane (2000), Penrose Deccan 2000, in *Proceedings of the Field Excursion Guide to the Western Deccan Basalt Province, Penrose Field Guides*, p. 241, Geol. Soc. of India, New Delhi.

Textor, C., H.-F. Graf, C. Timmreck, and A. Robock (2004), Emissions from volcanoes, in *Emissions of Atmospheric Trace Compounds*, edited by C. Granier, P. Artaxo, and C. E. Reeves, pp. 269–304, Dordrecht, Netherlands.

Thordarson, T. (2004), Sulfur emissions by flood lava emissions from basaltic eruptions, paper presented at European Geosciences Union 2004, Nice, France, 25–30 April.

Thordarson, T., and S. Self (1993), The Laki (Skaftár Fires) and Grímsvötn eruptions in 1783–1785, *Bull. Volcanol.*, *55*, 233–263.

Thordarson, T., and S. Self (1996), Sulfur, chlorine and fluorine degassing and atmospheric loading by the Roza eruption, Columbia River Basalt Group, Washington, USA, *J. Volcanol. Geotherm. Res.*, *74*, 49–73.

Thordarson, T., and S. Self (1998), The Roza Member, Columbia River Basalt Group: A gigantic pahoehoe lava flow field formed by endogenous processes?, *J. Geophys. Res.*, *103*, 27,411–27,445.

Thordarson, T., and S. Self (2003), Atmospheric and environmental effects of the 1783–1784 Laki eruption: A review and reassessment, *J. Geophys. Res.*, *108*(D1), 4011, doi:10.1029/2001JD002042.

Thordarson, T., S. Self, N. Óskarsson, and T. Hulsebosch (1996), Sulfur, chlorine, and fluorine degassing and atmospheric loading by the 1783–1784 AD Laki (Skaftár Fires) eruption in Iceland, *Bull. Volcanol.*, *58*, 205–225.

Vandamme, D. (1990), Apport du Paléomagnétisme à l'estimation de l'age, de la durée, de l'origine et des conséquences éventuelles du volcanisme des Traps du Deccan, Ph.D. thesis, 260 pp., Inst. de Phys. du Globe de Paris, Paris.

Vandamme, D., and V. Courtillot (1992), Paleomagnetic constraints on the structure of the Deccan Traps, *Phys. Earth Planet. Inter.*, *74*, 241–261.

Vandamme, D., V. Courtillot, J. Besse, and R. Montigny (1991), Paleomagnetism and age determinations of the Deccan Traps (India): Results of a Nagpur-Bombay traverse and review of earlier work, *Rev. Geophys.*, *29*, 159–190.

Venkatesan, T. R., K. Pande, and K. Gopalan (1993), Did Deccan volcanism pre-date the Cretaceous/Tertiary transition?, *Earth Planet. Sci. Lett.*, *119*, 181–189.

Venkatesan, T. R., K. Pande, and Z. G. Ghevariya (1996), ^{40}Ar-^{39}Ar ages of lava flows from Anjar, Western Deccan Province, India and its relation to the Cretaceous-Tertiary Boundary events, *Curr. Sci.*, *70*, 990–996.

Verati, C., C. Rapaille, G. Féraud, A. Marzoli, H. Bertrand, and N. Youbi (2007), ^{40}Ar/^{39}Ar ages and duration of the central Atlantic magmatic province volcanism in Morocco and Portugal and its relation to the Triassic-Jurassic boundary, *Palaeogeogr. Palaeoclimatol. Palaeoecol.*, *244*, 308–325.

Wensink, H., and C. T. Klootwijk (1971), Paleomagnetism of the Deccan Traps in the Western Ghats near Poona (India), *Tectonophysics*, *11*, 175–190.

White, R. V., and A. D. Saunders (2004), Volcanism, impact and mass extinctions: Incredible or credible coincidences?, *Lithos*, *79*(3–4), 299–316.

Widdowson, M., and K. G. Cox (1996), Uplift and erosional history of the Deccan Traps, India; evidence from laterites and drainage patterns of the Western Ghats and Konkan coast, *Earth Planet. Sci. Lett.*, *137*, 57–69.

Widdowson, M., N. Walsh, and K. V. Subbarao (1997), The geochemistry of Indian bole horizons: Palaeoenvironmental implications of Deccan intravolcanic palaeosurfaces, in *Palaeosurfaces: Recognition, Reconstruction, and Paleoenvironmental Interpretation*, edited by M. Widdowson, *Geol. Soc. Spec. Publ.*, *120*, 221–248.

Wignall, P. B. (2001), Large igneous provinces and mass extinctions, *Earth Sci. Rev.*, *53*, 1–33.

Wilkins, A., K. V. Subbarao, G. Ingram, and J. N. Walsh (1994), Weathering regimes within the Deccan Basalts, in *Volcanism*, edited by K. V. Subbarao, pp. 217–231, Wiley Eastern, New Dehli.

Yang, W., and T. J. Ahrens (1998), Shock vaporization of anhydrite and global effects of the K-T bolide, *Earth Planet. Sci. Lett.*, *156*, 125–140.

Zijderveld, J. D. A. (1967), A. C. demagnetization rocks-analysis of results, in *Methods in Paleomagnetism*, edited by D. W. Collinson, K. M. Creer, and S. K. Runcorn, pp. 254–286, Elsevier, Amsterdam.

A.-L. Chenet, V. Courtillot, and F. Fluteau, Laboratoire de Paléomagnétisme, Insitut de Physique du Globe de Paris, T14-15 2ème étage, Case courrier 089, 4 place Jussieu, F-75252 Paris Cedex 05, France. (alchenet@ipgp.jussieu.fr)

M. Gérard, Département de Minéralogie, IMPMC, 140 rue de Lourmel, F-75015 Paris, France.

K. V. Subbarao, Centre for Earth Science and Space Sciences, University of Hyderabad, Gachibowly, Hyderabad, 500046, India.